ANKZF1 helps to eliminate the stress-damaged mitochondria by LC3-mediated mitophagy

Mudassar Ali[1] and Koyeli Mapa[1*]

1. Protein Homeostasis Laboratory, Department of Life Sciences, School of Natural Sciences, Shiv Nadar Institution of Eminence, Delhi-NCR, Greater Noida, Gautam Buddha Nagar, Uttar Pradesh 201314, India.

* Correspondence: koyeli.mapa@snu.edu.in

Keywords: Mitochondria, Mitophagy, proteotoxic stress, PINK, Parkin, LC3

Running Title: ANKZF1 interacts with LC3 to clear damaged mitochondria

Abstract

Mitochondria, the double membrane-bound organelles of endosymbiotic origin, are crucial centers for cellular energy production and several essential metabolic pathways. Recent studies reveal that mitochondria become dysfunctional following numerous cellular stresses, and during pathologies, demanding an extensive investigation of mitochondrial turnover mechanisms. Apart from the specific response pathways to tackle different stresses, mitophagy or degradation of mitochondria by autophagy is a critical quality control mechanism that clears irreversibly damaged mitochondria. Mitophagy is majorly executed either by receptor-mediated or PINK-Parkin-dependent pathways. Here, we show that the human orthologue of yeast Vms1, ANKZF1, participates in PINK-Parkin-mediated mitophagy. We show that ANKZF1 is extensively recruited to damaged mitochondria along with Parkin during mitochondrial proteotoxic stress induced by the expression of a single misfolded/aggregated protein or during uncoupler-induced membrane depolarization. Importantly, ANKZF1 recruitment to damaged mitochondria is significantly enhanced in the presence of Parkin, and ANKZF1 physically interacts with Parkin and LC3 during mitochondrial proteotoxic or depolarization stresses. ANKZF1 harbors six putative LC3-interacting regions (LIRs), LIR4 present at residues 333-336 is particularly important for ANKZF1-LC3 interaction. Furthermore, we show that *ANKZF1* knockout cells are compromised in clearing stress-damaged mitochondria by mitophagy, indicating an important role of ANKZF1 in mitochondrial turnover during stress. In summary, we show a new role of ANKZF1 in eliminating the stress-damaged mitochondria, reiterating the mito-protective role of Vms1/ANKZF1 during mitochondrial stresses.

Introduction

Understanding organelle homeostasis under different cellular stresses has become one of the key areas of research in modern biology. Mitochondria is a major sub-cellular organelle that is frequently damaged and becomes dysfunctional during various cellular stresses and pathological conditions. Such stresses affect mitochondrial dynamics and functions, necessitating the elimination of damaged mitochondria and the subsequent biogenesis of new mitochondria to maintain the required pool of functional mitochondria in the cell.

Various small molecule stressors have been employed to induce mitochondrial stress to understand the response to such stresses. Mitochondrial membrane depolarizing agents like CCCP (Carbonyl Cyanide m-ChloroPhenylhydrazone) [1, 2], specific respiratory chain blockers e.g. rotenone [3, 4], oligomycin, antimycin, mitochondrial DNA damaging agents like ethidium bromide (EtBr) [5], or oxidizing agents that produce Reactive Oxygen Species (ROS) e.g. paraquat [1], H_2O_2 [4, 6, 7] have been extensively used as mitochondrial stressors. In some studies, specific mutant mitochondrial proteins were expressed within the organelle to understand the response pathways to mitochondrial protein misfolding or proteotoxic stresses. In some recent studies, protein import to mitochondria was blocked to induce stress in the organelle [8]. Many such studies revealed the existence of novel response pathways to manage stress in and around mitochondria. Recent works in yeast, *Saccharomyces cerevisiae,* revealed discoveries of pathways like Mitochondrial Compromised Protein import Response (mitoCPR) [9], Mitochondrial Translocation Associated Degradation (mitoTAD) [10], Unfolded Protein Response activated by mistargeting of proteins (UPRam) [11-14], early mitoUPR [15], and Mitochondria Associated Degradation (MAD) [16, 17] etc. In metazoans like *C. elegans* and mammalian systems, the commencement of mitochondrial Unfolded Protein Response (mitoUPR) was reported upon DNA damage-induced stress [5] and proteotoxic stress, respectively. Recently, the contribution of the Ribosome Quality Control (RQC) pathway was shown to be vital for the

protection of mitochondria from RQC byproducts like CAT (C-terminal Alanine Threonine extension)-tailed precursor proteins [18-20].

In case of overwhelming stress, damaged mitochondria are cleared by mitophagy. Upon activation, mitophagy is initiated by the dedicated receptor proteins forming phagophores. Mitophagy receptors or autophagy adaptor proteins initiate the phagophore formation by interacting with the Atg8-family of proteins like LC3 (Microtubule-associated protein 1A/1B-light chain 3) or GABARAPs (Gamma-Amino-Butyric Acid type 1 Receptor) present in the phagophore membrane that in turn initiate the autophagosome formation surrounding the damaged organelle. These phagophores ultimately encircle the damaged mitochondria, forming autophagosomes, and subsequently fuse to lysosomes forming autophago-lysosomes. Within the autophago-lysosomes, the lysosomal hydrolytic enzymes digest the engulfed material.

PTEN-Induced putative Kinase protein 1 (PINK1) is involved in an alternate pathway of mitochondrial quality control and clearance [21-24]. Whenever PINK1 senses the mitochondrial membrane damage, it accumulates on the outer mitochondrial membrane where it further recruits Parkin, an E3 ubiquitin ligase from cytosol [1, 22, 25]. PINK1 phosphorylates ubiquitin and activates the E3 ubiquitin ligase activity of Parkin, which further governs the polyubiquitination of various outer mitochondrial membrane proteins on damaged mitochondria. These polyubiquitinated proteins are sensed by mitophagy adapter proteins, which act as a bridge between damaged mitochondria and autophagosomes. The adaptor proteins interact with polyubiquitinated proteins via their ubiquitin-associated (UBA) domain, on the other hand, they also interact with LC3 present on the phagophore membrane via the LIR (LC3 Interacting region) motif. These associations lead to the encircling of the damaged mitochondria by phagophores forming autophagosomes followed by clearance of the damaged organelle.

ANKZF1 (Ankyrin repeat and Zinc Finger Peptidyl tRNA Hydrolase 1) is the mammalian orthologue of Vms1 protein of yeast, *Saccharomyces cerevisiae.* Previous literature shows

its involvement in the Ribosome Quality Control (RQC) pathway [26-29], where it acts as a tRNA hydrolase and recycles the nascent peptides from stalled ribosomes [26, 27, 29]. Importantly, Vms1 was shown to balance the CAT-tailing activity by RQC component Rqc2 and hence decreases the chance of import of CAT-tailed mitochondrial precursor proteins to the organelle reducing the chance of aggregation of CAT-tailed proteins within mitochondria [18-20]. Other studies showed the involvement of Vms1 in the recruitment of ubiquitin-proteasome system component Cdc48/VCP on damaged mitochondria during oxidative stress, to facilitate the Mitochondria-Associated-Degradation (MAD) pathway [16, 30, 31]. Interestingly, it was shown that during H_2O_2-induced oxidative stress, both Vms1 and ANKZF1 are localized to mitochondria although the necessity of mitochondrial localization of these proteins remains elusive [31, 32]. Recently, we have shown the specific modulatory role of *VMS1* during proteotoxic stress in the mitochondrial matrix in yeast. We showed that deletion of *VMS1* leads to aggravation of proteotoxicity in the mitochondrial matrix [33]. All these findings highlight the crucial roles of Vms1 during mitochondrial stress.

In the current study, we explored the role of the human protein ANKZF1 in mitochondrial stresses. We show that, during single misfolded-protein-induced mitochondrial proteotoxic stress or depolarization stress by CCCP treatment, ANKZF1 associates with mitochondria and co-localizes with Parkin. ANKZF1 also shows interaction with LC3 during mitochondrial stresses. Furthermore, sequence analysis of the protein revealed the presence of six putative LIR motifs; out of these six LIRs, LIR-4 harbored at amino acid residues 333-336 is indispensable for LC3-interactions. Lastly, knockout cells of *ANKZF1* exhibited compromised clearance of stress-damaged mitochondria by mitophagy. Taken together, our study shows an important aspect of ANKZF1 in mitochondrial homeostasis; it plays an important role in the clearance of damaged mitochondria by LC3-mediated mitophagy during proteotoxic stress or depolarization stress of the organelle.

Results

ANKZF1 efficiently recruits to mitochondria during certain chemical-induced stresses in the organelle exclusively in the presence of Parkin

ANKZF1 is a multi-domain protein like its yeast orthologue, Vms1 (Figure 1A). To check any role of ANKZF1 in mitochondrial stresses, we expressed a C-terminally Green Fluorescent Protein (GFP) tagged version of the protein in HeLa cells and analyzed its cellular localization using imaging by confocal microscopy upon treatment with different mitochondrial stressors. In unstressed cells, ANKZF1-GFP does not show any distinct co-localization (Figure 1B) with the mitochondrial network. In the presence of various small molecule mitochondrial stressors like sodium Azide, H_2O_2, paraquat, rotenone, rapamycin and CCCP, there was no noticeable mitochondrial localization or recruitment of ANKZF1 on the mitochondrial network (Figure 1C).

CCCP treatment is known to cause mitochondrial stress and induce mitophagy majorly mediated by the PINK1-Parkin pathway [22, 35, 36]. As HeLa cells express Parkin at an insignificant level, we overexpressed Parkin with N-terminally-tagged mCherry and observed its association with mitochondria during chemical-induced mitochondrial stresses, as described above. As reported earlier, Parkin shows significant overlap with fragmented mitochondria post-CCCP treatment indicating recruitment of mitophagy apparatus on the depolarized and fragmented mitochondria (Figure 1D, middle column) [22]. Interestingly, when we co-expressed ANKZF1-GFP with Parkin, it showed significant co-localization with mCherry-Parkin indicating an interaction of ANKZF1 with Parkin (Figure 1D, middle column, and Figure 1E). This result reiterates the previously reported physical interaction between Parkin and ANKZF1 [37]. Similarly, upon rapamycin treatment, Parkin overlaps with the fragmented mitochondrial network, and ANKZF1 and Parkin are co-localized with fragmented mitochondria (Figure 1D, right column, and Figure 1E). With other stressors (rotenone, sodium-azide, H_2O_2 and paraquat), Parkin recruitment to the mitochondrial

network remains insignificant, and ANKZF1 co-localization with mitochondria is not significant (Figure S1A).

To assess whether the mitochondrial membrane-depolarization is the key determinant of Parkin recruitment to the stressed mitochondria, we imaged the uptake of the mitochondrial membrane potential-dependent fluorescent dye, TetraMethylRhodamine Ethyl ester (TMRE) [38], by mitochondria. Untreated mitochondria exhibited a bright TMRE signal completely overlapping with the mitochondrial network indicating intact mitochondrial membrane potential, as expected (Figure S1B, topmost row). CCCP treatment significantly diminished the TMRE uptake due to membrane depolarization (Figure S1B, second row from top and S1C). Other stressors like rapamycin, rotenone, paraquat and sodium-azide also showed significantly decreased uptake of TMRE, albeit less prominent than CCCP treatment, indicating defects in the maintenance of membrane polarization upon treatment with these compounds (Figure S1B and S1C). Notably, treatment with H_2O_2 showed normal TMRE uptake like untreated healthy cells (Figure S1B and S1C). Although most of these stressors led to membrane depolarization, at least partially, and mitochondrial fragmentation, Parkin and ANKZF1 recruitment to mitochondria were not significant. This result hints that the interaction between Parkin/ANKZF1 and mitochondria is stress specific.

Proteotoxic stress due to expression of mitochondria-targeted misfolded proteins leads to severe mitochondrial fragmentation and may lead to depolarization

We have recently shown that yeast Vms1 plays an important modulatory role during mitochondrial matrix proteotoxic stress [33]. To investigate the role of the mammalian orthologue of Vms1, ANKZF1, during mitochondrial proteotoxic stress, we developed a mitochondria-specific proteotoxic stress model in human cells. To impart proteotoxic stress exclusively to mitochondria, we targeted two exogenous model misfolded proteins: i) Parkinson's disease-associated A53T mutant of α-synuclein (referred to as A53T-Syn hereafter) [39, 40] and ii) recently described amyloid-forming aggregation-prone protein,

PMD (Protein with Misfolded Domains) [33], to mitochondria. Specific targeting of model proteins was achieved using the Mitochondrial Targeting Signal (MTS) of SMAC (Second Mitochondria-derived Activator of Caspase) (Figure 2A) and the proteins were expressed as fusion proteins with a C-terminal GFP tag (Figure 2A). Confocal microscopy of the GFP-tagged proteins reveals complete overlap with the signal of the Mito-mCherry, indicating correct localization of the stressor proteins to mitochondria (Figure 2B and 2C). Mitochondria-targeted GFP, without any fused stressor proteins, serves as the control of overexpression of exogenous proteins within mitochondria. As reported before, PMD protein forms prominent amyloids in vitro [33]. When expressed within mitochondria, the protein forms SDS-insoluble aggregates and it is difficult to detect the expression of the protein by western blot using the standard method of denaturation for sample loading (Figure S2A). With exclusive use of lysis buffer containing a strong denaturant like 8M urea, PMD aggregates are solubilized, and the protein is detectable by western blot at the expected size indicating formation of the SDS-insoluble aggregates by the protein in mitochondria (Figure S2B). A53T-Syn is detected by standard western blot techniques at the expected size (Figure S2A). Expression of both the stressor proteins leads to increased fragmentation of the mitochondria as evidenced by a significant reduction in the mitochondrial branch length (Figure 2B, 2D and 2E), more prominently in the case of PMD protein-induced proteotoxic stress (Figure 2B, 2D and 2E).

Next, we investigated the mitochondrial membrane potential after imparting the proteotoxic stress, Mitochondrial TMRE uptake remained mostly unaffected in mitochondria expressing A53T-Syn mutant protein indicating intact membrane polarization despite stress due to expression of this protein (Figure S2C and S2D). In contrast, expression of PMD protein in mitochondria led to severe depolarization (like CCCP treatment as shown in Figure S2C, lowermost rows) as indicated by significant defects in the uptake of TMRE compared to the control cells (Figure S2C and S2D). This data indicated that the extent of stress and its effect on the mitochondrial forms and function depends on the property of the misfolded protein.

ANKZF1 interacts with mitophagy/autophagy machinery during proteotoxic stress in mitochondria

As proteotoxic stress leads to severe mitochondrial fragmentation as well as depolarization with PMD-induced stress, we went ahead to check whether the fragmented and damaged mitochondria are cleared by the autophagy pathway. First, we took the tandemly fluorescently tagged-LC3 (tfLC3) tagged with monomeric RFP (Red Fluorescent Protein) followed by GFP (Green Fluorescent Protein) [41](Figure 3A) as a reporter protein. When we performed imaging of the tfLC3 using confocal microscopy in the control non-stressed cells, very few LC3 puncta were visible with both green and red fluorescence which completely overlap with each other upon merging the images from both the channels [same number of puncta in the red channel and merged (yellow) channel] (Figure 3A, top row). When we co-expressed the tfLC3 with the mitochondrial stressor proteins (either A53T-Syn or PMD), the number of LC3 puncta increased (Figure 3A, middle and lower rows) compared to the control condition (Figure 3A, top row). Notably, the number of LC3 puncta is prominently more in PMD-protein induced stress compared to stress due A53T-Syn expression, again indicating differential stress response depending on the nature of the protein that misfolds or aggregates within mitochondria. Interestingly, apart from the increased number of LC3 puncta, the number of puncta exclusively with RFP fluorescence was significantly high during proteotoxic stress (Figure 3A, middle and lower rows and Figure 3B). This data indicated that proteotoxic stress in mitochondria leads to increased bulk autophagy.

As described earlier that Parkin is one of the key regulators of PINK1/Parkin-mediated mitophagy, we monitored Parkin puncta recruitment to mitochondria to understand the extent of clearance of the damaged mitochondria during proteotoxic stress in the organelle by mitophagy. Upon expressing the stressor proteins, A53T-Syn or PMD, Parkin showed punctate structures mostly co-localized with the mitochondrial network (Figure S3A, middle and bottom rows), however in unstressed cells, Parkin exhibits diffused cytosolic localization

(Figure S3A, top row). The extent of Parkin puncta co-localized to the mitochondrial network was more prominently visible during PMD-induced mitochondrial proteotoxic stress (Figure S3A, bottom row).

Upon checking the ANKZF1 cellular distribution (in the absence of Parkin) during mitochondrial proteotoxic stress, we found some punctate localization of ANKZF1 during stress (Figure 3C, middle and bottom rows) in contrast to diffused cytosolic localization of the protein in the control cells (Figure 3C, upper row). This was in contrast to chemical-induced stresses where the protein does not recruit to mitochondria at all, in the absence of Parkin. Upon overexpression of Parkin, ANKZF1 recruitment on mitochondria during proteotoxic stress was significantly increased (Figures 3D, 3E and 3F). As previously shown in the case of CCCP treatment, during proteotoxic stress also, ANKZF1 and Parkin puncta showed significant co-localization (Figures 3D and 3E). As ANKZF1 showed strong interaction with Parkin in multiple mitochondrial stresses, it indicated a possible role of the protein in the process of mitophagy.

To check the association of ANKZF1 with other players of mitophagy, its interaction with other components was further checked. During proteotoxic stress in mitochondria, ANKZF1 puncta showed significant co-localization with LC3 puncta over fragmented mitochondria (Figures 4A and 4B) reiterating its association with mitophagy/autophagy components. Co-expression of ANKZF1, Parkin and LC3 in the cells experiencing PMD-induced stress in mitochondria, shows complete co-localization of ANKZF1 with Parkin and LC3 in a ring-like structure (Figure 4C, lower panels). Interestingly, all three proteins are co-localized to each other during mitochondrial proteotoxic stress. This association was further checked for endogenous ANKZF1 protein, cells were co-transfected with Mito-PMD-BFP, GFP-Parkin and RFP-LC3 followed by ANKZF1 immuno-staining with anti-ANKZF1 antibody. In this case too, images show similar pattern of co-localized events of Parkin, LC3 and ANKZF1 during proteotoxic stress (Figure S4A). Furthermore, to determine the physical interaction of ANKZF1 with Parkin and LC3 during mitochondrial proteotoxic stress (by expressing PMD)

and depolarization, we performed co-immunoprecipitation experiments. HEK293T cells were transfected with ANKZF1-GFP and mCherry-Parkin having mitochondrial stress due to expression of PMD or due to CCCP treatment. Mito-BFP was used as a control of exogenous folded protein overexpression in mitochondria. Importantly, Parkin was exclusively co-precipitated with anti-GFP antibody, indicating a physical interaction between ANKZF1-GFP and Parkin during PMD-induced proteotoxic stress as well as mitochondrial depolarization stress due to CCCP treatment (Figure 4D, Figure S8). In the control condition (with Mito-BFP expression), no interaction of Parkin and ANKZF1 was observed. Endogenous LC3 was precipitated with ANKZF1-GFP during PMD-induced proteotoxic stress and during CCCP-induced stress (Figure 4D, Figure S8), indicating an interaction between LC3 and ANKZF1, as observed by imaging experiments. Furthermore, ANKZF1's interaction with lysosome was also checked during proteotoxic stress. ANKZF1 showed a significant co-localization with lysosomal protein LAMP1, suggesting fusion of ANKZF1-containing autophagosomes with lysosomes indicating the role of the protein in mitophagy (Figure S4B).

ANKZF1 possesses features of mitophagy adaptor proteins

ANKZF1's interaction with Parkin and LC3 during mitochondrial stresses (proteotoxic and depolarization) indicated its possible role as a mitophagy adaptor protein. As reported before, all mitophagy receptor or autophagy adaptor proteins harbor a particular amino acid sequence consisting of aromatic amino acids (W/Y/F) followed by any two amino acids (XX) and end with an aliphatic amino acid (L/I/V) [42]. These regions of the autophagy/mitophagy adaptor proteins are known as LC3-Interacting Region (LIR) [43-46]. When we checked the human mitophagy receptor/adaptor proteins, NIX, BNIP3, p62, optineurin, or AMBRA1, we found the conserved LIR motif in all the known mitophagy receptor/adaptors, as expected (Figure 5A). Interestingly, we found six such LIR motifs in the human ANKZF1 protein sequence (Figure 5B). After multiple sequence analyses of ANKZ1 sequences of different

mammals, we found most of them contain multiple such conserved LIR sequences (Figure 5C). To check the importance of these predicated LIRs for ANKZF1-LC3 interaction, we first made three truncation mutants of ANKZF1; Δ210-ANKZF1 (containing deletion of N-terminal 210 amino acids), Δ330-ANKZF1 (containing deletion of N-terminal 330 amino acids) and Δ370-ANKZF1 (containing deletion of N-terminal 370 amino acids) (Figure 5D). As shown in Figure 5D, Δ210 mutant is devoid of LIR-1 and LIR-2, Δ330 mutant is deleted of LIR-1, LIR-2 and LIR-3. Δ370 mutant lacks the first 5 LIRs (LIR-1 to LIR-5) and contains only the LIR-6 (495th-498th residues). Interestingly, Δ210-ANKZF1 and Δ330-ANKZF1 truncation mutants retain the co-localization with LC3 puncta, like wild-type ANKZF1 protein during PMD-induced stress in the mitochondria (Figures 5E, 5F), suggesting that LIR-1, LIR-2 and LIR-3 are dispensable for interaction with ANKZF1. In contrast, Δ370-ANKZF1 did not show any punctate structure co-localized with LC3 during the same stress, indicating an important role of LIR-4, LIR-5 and LIR-6 in LC3 interaction (Figures 5E, 5F). This experiment was recapitulated in SHSY-5Y cells and similar findings were observed (Figure S5A)

Furthermore, to confirm the exact LIR required for LC3 interaction, we generated point mutations by site-directed mutagenesis in the LIR-4, LIR-5 and LIR-6. We mutated the W/Y/F and L/I/V residues to Alanine. Thereafter, the co-localization of mutant ANKZF1 with LC3 was analyzed during PMD-induced proteotoxic stress. Notably, mutating the LIR-5 and LIR-6 of ANKZF1 did not abolish its interaction with LC3. However, LIR-4 (amino acids 333-336) mutant showed no co-localized events between ANKZF1 and LC3 (Figure 5G). This result indicates the importance of LIR-4 (333 FQEL 336) in the interaction with autophagophores. Thus, LIR-4 is the critical LIR motif in the ANKZF1 required for interaction with LC3 to facilitate mitophagy.

We further checked the interaction of LIR-4 mutant of ANKZF1 with Parkin during proteotoxic stress and found that both proteins are co-localized (Figure S5B). Thus, LIR 4 is specifically required for interaction with LC3.

To fulfill the criteria of the mitophagy adaptor protein, ANKZF1 must contain a ubiquitin-associated domain (UBA). We checked the ANKZF1 interaction with ubiquitin during PMD-induced stress and found ANKZF1 puncta co-localizes with Ub-DsRed puncta, suggesting that it possesses a ubiquitin-binding motif (Figure S5C). However, this result requires further characterization to understand the exact position of the UBA domain in ANKZF1.

ANKZF1 knockout (KO) cells are specifically defective in mitophagy, but bulk cellular autophagy remains unaffected

To check any impairment in autophagic clearance of damaged mitochondria in the absence of ANKZF1, we generated the CRISPR-Cas9 mediated knockout of *ANKZF1* in HeLa cells (Figures 6A and 6B). For all experiments, two clones of *ANKZF1* KO cells (clone 1 and clone 2) were used (Figure 6B, Figure S8). To assess any alterations in mitophagy in the absence of ANKZF1, we utilized the Mito-Keima (Mt-Keima) reporter described before [47-49], in the *ANKZF1* KO cells. Mt-Keima was co-expressed along with control protein or stressor protein PMD in mitochondria of WT HeLa cells and *ANKZF1* KO cells to evaluate any alterations in the mitophagy events in the absence of ANKZF1. The images of Mt-Keima captured at 488 nm excitation and 640 nm emission are depicted in green and the images taken after excitation at 560 nm and emission at 640 nm are shown in red (Figure 6C). In WT HeLa cells, as expected, the average mitophagy events (red signal to green signal ratio) during mitochondrial proteotoxic stress (due to expression of PMD) were found to be extremely high (Figure 6C and S6B, 2nd row from top) in comparison to the non-stressed control cells (Figure 6C and S6B, uppermost row). Although *ANKZF1* KO cells also showed higher mitophagy events during PMD-induced mitochondrial stress (Figures 6C and S6B, third and fourth rows from top), when we compared the shift of Keima488 to Keima560 (change of mitochondrial pH from basic/neutral to acidic), we found significant difference between WT and KO cells, suggesting reduced mitophagy in KO cells (Figure 6D and S6C). However, this change was reverted to WT level when ANKZF1 was overexpressed in the KO cells (Figure

S6D). Also, the average number of mitophagy events between WT and KO cells expressing PMD, we observed a significant reduction in the average mitophagy events in the KO cells (Figure 6E). We further checked if cells lacking *ANKZF1* are impaired in bulk autophagy or not, we used the tf-LC3 reporter as described in the earlier sections. For that purpose, tf-LC3 was expressed with either control mito-BFP or mito-PMD protein in WT and KO cells. Increased autophagy was observed after PMD expression compared to control cells (Figure S6A). However, no significant difference in bulk autophagy was observed between WT and *ANKZF1* KO cells (Figure S6A) suggesting ANKZF1 is specifically important for mitophagy but not for bulk autophagy.

Next, alterations in mitophagy events were also checked in *ANKZF1* KO cells by inducing mitochondrial depolarization by CCCP treatment. The ratio of Mt-Keima fluorescence emission after excitation at 560nm with the emission after excitation at 488 nm was used as a surrogate for ongoing mitophagy as described before. In WT cells, CCCP treatment led to an increase in the ratio due to increased mitophagy (Figure S7A, top two rows). In the *ANKZF1* KO cells, Mt-Keima ratio was significantly reduced compared to WT cells following CCCP treatment indicating ineffective mitophagy in the absence of ANKZF1 (Figures S7A, and S7B).

In summary, we show that absence of ANKZF1 leads to significant reduction in mitophagic clearance of stress-damaged mitochondria although the bulk cellular autophagy remains unaltered in absence of the protein. Thus, ANKZF1 acts as a specific adaptor for mitophagy to clear out irreversibly damaged mitochondria.

Discussion

Mitophagy or specific clearance of damaged mitochondria by the process of autophagy, is a complex multi-step process involving several components. In PINK-Parkin-dependent pathway, usually the depolarized mitochondria accumulate non-translocated PINK1 on the

mitochondrial surface, which helps in recruitment of Parkin, an E3 ubiquitin ligase on mitochondrial outer membrane. Parkin helps in poly-ubiquitination of outer mitochondrial membrane proteins, which interact with the mitophagy adaptor/receptor proteins. These adaptor and receptor proteins act as bridges between the mitochondrial outer membrane and LC3 on the growing phagophore membrane, thus facilitating the encircling of the damaged mitochondria by isolation membranes, ultimately forming autophagosomes. Thus, mitophagy adaptor proteins are crucial players in the whole course of autophagic clearance of mitochondria from the early steps of the process. So far, many mitophagy adaptor proteins have been discovered, some of these proteins have been identified only recently.

In this study, we show that human ANKZF1, an orthologue of yeast Vms1, acts as a mitophagy adaptor protein. We show that ANKZF1 recruits to mitochondria when some small molecule stressors are used to exert stress in the organelle. Among the chemical stressors used, treatment with mitochondrial depolarizing agents like CCCP or treatment with rapamycin caused significant recruitment of ANKZF1 to mitochondria. Interestingly, ANKZF1 recruitment to mitochondria was significant exclusively in the presence of Parkin with which it shows prominent co-localization and physical interaction. ANKZF1 was also found to be co-localized with LC3 during CCCP and rapamycin-induced stress, suggesting that during mitochondrial stress ANKZF1 interacts with autophagosome.

Apart from the chemical stress, we have imparted specific proteotoxic stress to mitochondria by expressing model misfolded and aggregation-prone proteins within the organelle. Here, we established that expression of model aggregation-prone proteins inside mitochondria lead to severe mitochondrial fragmentation and loss of membrane potential with specific aggregated proteins like PMD, which is sufficient to activate the clearance of damaged mitochondria by mitophagy. It is noteworthy to mention that some misfolded and aggregation prone proteins (like A53T-Syn) do not cause membrane depolarization, yet the stress imparted to mitochondria by these proteins are sufficient to send signals for the onset of mitophagy.

While investigating the role of ANKZF1 during depolarization-induced or proteotoxic-stress-induced mitochondrial damage, we found that the ANKZF1 shows interesting punctate localization with the mitochondrial network quite prominently in the presence of Parkin. A series of imaging experiments showed ANKZF1 and Parkin co-localized with each other in response to stress in mitochondria. As stated previously, Parkin overexpression increases the ANKZF1 localization and puncta formation during mitochondrial stress suggesting ANKZF1 recruitment is a Parkin-dependent event and is a downstream process of Parkin recruitment, . This result prompted us to check its role as mitophagy adaptor proteins. Furthermore, ANKZF1 co-localization with LC3 intensified the chance of the protein acting in the mitophagy pathway. Indeed, we found features of mitophagy adaptor proteins present in the ANKZF1 sequence. ANKZF1 sequence shows six possible LIR motifs among which the fourth LIR shows indispensability for interaction with LC3 although when the localization with Parkin was checked, ANKZF1 mutant showed no change and co-localized like wild-type proteins with Parkin. Importantly, we have further shown that *ANKZF1* KO cells are compromised in the clearance of damaged mitochondria by mitophagy reiterating the importance of this protein in mitophagy. We have summarized the role of ANKZF1 as mitophagy adaptor protein in Figure 7. In summary, we have shown a new function of ANKZF1 in clearing stress-damaged mitochondria by LC3-mediated mitophagy. We have convincingly shown the presence and position of critical LIR in the protein and its interaction with LC3. We have also shown its interaction with ubiquitin, the two major properties by which the mitophagy adaptor proteins are characterized, although we could not decipher the exact position of the ubiquitin-binding domain of the protein. This finding reiterates the importance of this protein in the protection of mitochondria in various ways, either acting in the mito-RQC pathway or as a mitophagy adaptor protein.

The bigger question of the requirement of an additional mitophagy adaptor from cytoplasm remains elusive, currently. The triggering factor for ANKZF1 recruitment to damaged mitochondria remains to be explored in the future.

Material and Methods

Cell Culture, Transfection and Treatments

HeLa and HEK293T cells were cultured in DMEM (low glucose) containing 10% FBS (Gibco) and maintained at 37°C with 5% CO_2. SHSY-5Y cells were cultured in 45% DMEM, 45% Ham's F-10 media supplemented with 10% FBS, and maintained at 37°C with 5% CO_2. All transfection of plasmid DNA in HeLa and SHSY-5Y cells was done by lipofectamine 2000™ (Invitrogen) and polyethylenimine (PEI) was used for plasmid transfection in HEK293T cells using the manufacturer's recommended protocols. Cells were administered with 30µM, 60µM, and 90µM of the uncoupler Carbonyl Cyanide m-ChloroPhenyl hydrazone (CCCP) to disrupt the mitochondrial membrane potential. To induce bulk autophagy, cells were treated with 200nM Rapamycin for 24 hours. To increase the cellular ROS production, cells were treated with 2mM Paraquat or 1mM H_2O_2 for 12 hours and 2 hours respectively. To induce mitochondrial damage, cells were treated with 5µM rotenone for 4 hours and 5mM Sodium Azide for 3 hours. To stain the mitochondria, cells were treated with 200nM MitoTracker deep red for 30 minutes before imaging.

Plasmids and Cloning

Constructs used in this study include the following: EBFP2-N1 (Addgene, # 54595), mCherry Parkin (Addgene), mCherry-Mito-7 (Addgene #55102), ptfLC3 (Addgene #21074), Mito GFP, RFP-LC3, pHAGE-mt-mKeima (Addgene #131626). ANKZF1-FL-GFP, Δ210-ANKZF1-GFP, Δ330-ANKZF1-GFP, and Δ370-ANKZF1-GFP constructs were generated by using standard restriction digestion-based molecular cloning technique, and desired genes were ligated with digested pEGFPN1 (clonetech) empty vector backbone. ANKZF1 LIR mutants F333A-L336A, W366A-V369A, and W495A-L498A were generated by overlap-PCR based site-directed mutagenesis and cloned into pEGFPN1 vector. Mito-PMD-GFP construct was previously made in our lab and the cloning method was explained previously [33]. Mito-

A53T-α-Synuclein-GFP constructs were generated in the lab by using the same methodology where A53T α-synuclein gene was amplified from EGFP-alphasynuclein-A53T (Addgene #40823) and N-terminally fused with mitochondria targeting sequence of SMAC (Second Mitochondrial derived Activator of Caspase) by overlap PCR followed by the cloning of the overlapped fragment in digested pEGFPN1 vector. Mito-PMD-BFP and Mito-A53T-α-Synuclein-BFP constructs were generated by sub-cloning into EBFP2-N1 (addgene #54595). LAMP1 DsRed construct was generated by subcloning of LAMP1 from LAMP1-emiRFP670 (addgene #136570) into mCherryN1 plasmid backbone, plasmids were digested with XhoI and EcoRI restriction enzymes, followed by the ligation and transformation. Similarly, UbG76VdsRed construct was generated by subcloning of UbG76V from UbG76VGFP (addgene # 11941) into DsRedN1 vector backbone, both the vectors were digested with EcoRI and BamHI restriction enzymes, followed by the ligation and transformation by standard protocol.

Live Cell Imaging and Image Analysis

All microscopy images were acquired using an Apochromat 100X 1.4 NA oil immersion-based objective lens in a Nikon A1R MP+ Ti-E confocal microscope system. Imaging was performed at temperature (37°C), CO_2 (5%) and humidity controlled conditions. 405nm, 488nm, and 560nm lasers were used to excite the signals from BFP, GFP, and RFP/mCherry channels respectively, and the emission signals were detected by an automated du4 detector. mt-mKeima imaging was done by using the manual detector, where 488nm and 560nm lasers were used to excite the signals of neutral and acidic environments respectively, while both the emissions were collected at 620nm. Clearly visible ANKZF1 puncta and mt-mKeima puncta were manually counted in FIJI (NIH). TMRE and tf-LC3 fluorescence intensity and co-localization assessment were analysed and calculated in Nikon NIS Essentials analysis software. Mitochondria mean branch length was measured by using ImageJ plugin MiNa (mitochondrial network analysis).

Immunofluorescence Assay

Cells were seeded on the coverslip 24 hours before the transfection. Mito PMD-BFP, GFP-Parkin and RFP-LC3 were transfected, and cells were incubated for 24 hours. Next day, media were discarded, and cells were washed twice with 1XPBS and fixed with 4% formaldehyde at room temperature for 20 minutes, followed by permeabilization and blocking by 0.1% saponin and 10% FBS in 1XPBS solution for 1 hour at room temperature. After blocking, the primary anti-ANKZF1 antibody (1:100 dilution was prepared in the blocking solution) was added to the coverslip and incubated at room temperature for 1 hour, then cells were washed thrice with 1XPBS to remove any nonspecific binding. Lastly, secondary antibody Alexa 640 (1:1000 dilution was prepared in the blocking solution) was added for 1 hour at room temperature followed by washing and mounting the coverslip on the slide for imaging.

ANKZF1 Knockout cell line Generation

To target the ANKZF1 gene, sgRNA was designed by using an online server https://www.vbc-score.org/. Two separate guide RNA (5'-TCAAACAGGGAGATCGACGCAGG-3' and 5'-GCTTGGCCCGAACCGTATAGCGG-3') were selected based on the least off-target effects and high score to be effective as sgRNA. The sgRNAs were synthesized and cloned in pSpCas9 (BB)-2A-Puro (PX459) V2.0 (Addgene #62988) plasmid, followed by the transfection in HeLa cells. 24 hours post-transfection cells were supplemented with Puromycin (1µg/ml) for 48 hours, and selected cells were seeded in 96 well plates for the clonal population. Eventually, the surviving populations were screened and confirmed for knockout clones by ANKZF1-specific antibody by western blot.

Western Blot

Cells were lysed by RIPA buffer, protein amounts were quantified, and resolved in polyacrylamide gel electrophoresis and proteins were transferred to PVDF membrane. Membranes were blocked with 5% skimmed milk or 5% BSA dissolved in TBS-T, followed by the primary antibody and secondary antibody incubations. Lastly, blots were developed by using ECL reagents either in Protein Simple chemidoc system or using the x-ray films.

To detect the PMD protein, whole cell lysate was supplemented with 8M Urea in Laemmli buffer, and sample was heated at 80°C for 10 minutes before loading on gel and then standard western blotting protocol was followed as described above.

Multiple Sequence analysis

All the multiple sequence alignments were performed in Clustal Omega software and further confirmed in Tcoffee MSA server where protein sequences of the targeted proteins were submitted and checked for the aligned sequences.

Statistical analyses

All statistical analyses were performed either by using Microsoft Excel or by GraphPad Prism on the dataset of three independent repeats. Unpaired students t-test was performed to compare the dataset of two groups while for datasets with more than two groups one-way ANOVA with Dunnett multiple comparison test was performed, all error bars indicate mean± SEM.

Acknowledgements

KM acknowledges the funding support from the Science and Engineering Research Board (SERB), Government of India, for Core Research Grant (SERB/CRG/2022/006517) and SNIoE core funding. MA acknowledges the SNIoE PhD fellowship and fellowship from ICMR SRF Grant (2021-14421/CMB-BMS). MA and KM acknowledge the SNU DST-FIST grant

[SR/FST/LS-1/2017/59(c)] for the confocal microscopy facility. We thank Rajan Singh for his help at the confocal microscopy facility at SNIoE.

Author Contribution

The work was conceived by KM. Cell culture, molecular biology and imaging experiments were done by MA. Data were analysed by MA and KM. KM supervised the work; MA and KM wrote the manuscript.

Declaration of Financial Interest

The authors declare that there are no competing financial interests.

References

[1] Narendra D, Tanaka A, Suen DF, Youle RJ. Parkin is recruited selectively to impaired mitochondria and promotes their autophagy. J Cell Biol. 2008;183:795-803.
[2] Saita S, Shirane M, Nakayama KI. Selective escape of proteins from the mitochondria during mitophagy. Nat Commun. 2013;4:1410.
[3] Ahn BH, Kim HS, Song S, Lee IH, Liu J, Vassilopoulos A, et al. A role for the mitochondrial deacetylase Sirt3 in regulating energy homeostasis. Proc Natl Acad Sci U S A. 2008;105:14447-52.
[4] Frank M, Duvezin-Caubet S, Koob S, Occhipinti A, Jagasia R, Petcherski A, et al. Mitophagy is triggered by mild oxidative stress in a mitochondrial fission dependent manner. Biochim Biophys Acta. 2012;1823:2297-310.
[5] Nargund AM, Pellegrino MW, Fiorese CJ, Baker BM, Haynes CM. Mitochondrial import efficiency of ATFS-1 regulates mitochondrial UPR activation. Science. 2012;337:587-90.
[6] Zhang H, Kong X, Kang J, Su J, Li Y, Zhong J, et al. Oxidative stress induces parallel autophagy and mitochondria dysfunction in human glioma U251 cells. Toxicol Sci. 2009;110:376-88.
[7] Zhu H, Tamura T, Fujisawa A, Nishikawa Y, Cheng R, Takato M, et al. Imaging and Profiling of Proteins under Oxidative Conditions in Cells and Tissues by Hydrogen-Peroxide-Responsive Labeling. J Am Chem Soc. 2020;142:15711-21.
[8] Boos F, Kramer L, Groh C, Jung F, Haberkant P, Stein F, et al. Mitochondrial protein-induced stress triggers a global adaptive transcriptional programme. Nat Cell Biol. 2019;21:442-51.
[9] Weidberg H, Amon A. MitoCPR-A surveillance pathway that protects mitochondria in response to protein import stress. Science. 2018;360.
[10] Martensson CU, Priesnitz C, Song J, Ellenrieder L, Doan KN, Boos F, et al. Mitochondrial protein translocation-associated degradation. Nature. 2019;569:679-83.
[11] Callegari S, Dennerlein S. Sensing the Stress: A Role for the UPR(mt) and UPR(am) in the Quality Control of Mitochondria. Front Cell Dev Biol. 2018;6:31.
[12] Tran HC, Van Aken O. Mitochondrial unfolded protein-related responses across kingdoms: similar problems, different regulators. Mitochondrion. 2020;53:166-77.
[13] Wasilewski M, Chojnacka K, Chacinska A. Protein trafficking at the crossroads to mitochondria. Biochim Biophys Acta Mol Cell Res. 2017;1864:125-37.

[14] Wrobel L, Topf U, Bragoszewski P, Wiese S, Sztolsztener ME, Oeljeklaus S, et al. Mistargeted mitochondrial proteins activate a proteostatic response in the cytosol. Nature. 2015;524:485-8.
[15] Poveda-Huertes D, Matic S, Marada A, Habernig L, Licheva M, Myketin L, et al. An Early mtUPR: Redistribution of the Nuclear Transcription Factor Rox1 to Mitochondria Protects against Intramitochondrial Proteotoxic Aggregates. Mol Cell. 2020;77:180-8 e9.
[16] Heo JM, Livnat-Levanon N, Taylor EB, Jones KT, Dephoure N, Ring J, et al. A stress-responsive system for mitochondrial protein degradation. Mol Cell. 2010;40:465-80.
[17] Taylor EB, Rutter J. Mitochondrial quality control by the ubiquitin-proteasome system. Biochem Soc Trans. 2011;39:1509-13.
[18] Izawa T, Park SH, Zhao L, Hartl FU, Neupert W. Cytosolic Protein Vms1 Links Ribosome Quality Control to Mitochondrial and Cellular Homeostasis. Cell. 2017;171:890-903 e18.
[19] Kreft SG, Deuerling E. Vms1: A Cytosolic CAT-Tailing Antagonist to Protect Mitochondria. Trends Cell Biol. 2018;28:3-5.
[20] Lamech L, Haynes CM. Vms1 Relieves a Mitochondrial Import Chokehold. Dev Cell. 2017;43:259-60.
[21] Ashrafi G, Schwarz TL. The pathways of mitophagy for quality control and clearance of mitochondria. Cell Death Differ. 2013;20:31-42.
[22] Narendra DP, Jin SM, Tanaka A, Suen DF, Gautier CA, Shen J, et al. PINK1 is selectively stabilized on impaired mitochondria to activate Parkin. PLoS Biol. 2010;8:e1000298.
[23] Pickles S, Vigie P, Youle RJ. Mitophagy and Quality Control Mechanisms in Mitochondrial Maintenance. Curr Biol. 2018;28:R170-R85.
[24] Pickrell AM, Youle RJ. The roles of PINK1, parkin, and mitochondrial fidelity in Parkinson's disease. Neuron. 2015;85:257-73.
[25] Jin SM, Youle RJ. PINK1- and Parkin-mediated mitophagy at a glance. J Cell Sci. 2012;125:795-9.
[26] Kuroha K, Zinoviev A, Hellen CUT, Pestova TV. Release of Ubiquitinated and Non-ubiquitinated Nascent Chains from Stalled Mammalian Ribosomal Complexes by ANKZF1 and Ptrh1. Mol Cell. 2018;72:286-302 e8.
[27] Verma R, Reichermeier KM, Burroughs AM, Oania RS, Reitsma JM, Aravind L, et al. Vms1 and ANKZF1 peptidyl-tRNA hydrolases release nascent chains from stalled ribosomes. Nature. 2018;557:446-51.
[28] Yip MCJ, Keszei AFA, Feng Q, Chu V, McKenna MJ, Shao S. Mechanism for recycling tRNAs on stalled ribosomes. Nat Struct Mol Biol. 2019;26:343-9.
[29] Yip MCJ, Savickas S, Gygi SP, Shao S. ELAC1 Repairs tRNAs Cleaved during Ribosome-Associated Quality Control. Cell Rep. 2020;30:2106-14 e5.
[30] Heo JM, Nielson JR, Dephoure N, Gygi SP, Rutter J. Intramolecular interactions control Vms1 translocation to damaged mitochondria. Mol Biol Cell. 2013;24:1263-73.
[31] Nielson JR, Fredrickson EK, Waller TC, Rendon OZ, Schubert HL, Lin Z, et al. Sterol Oxidation Mediates Stress-Responsive Vms1 Translocation to Mitochondria. Mol Cell. 2017;68:673-85 e6.
[32] van Haaften-Visser DY, Harakalova M, Mocholi E, van Montfrans JM, Elkadri A, Rieter E, et al. Ankyrin repeat and zinc-finger domain-containing 1 mutations are associated with infantile-onset inflammatory bowel disease. J Biol Chem. 2017;292:7904-20.
[33] Narayana Rao KB, Pandey P, Sarkar R, Ghosh A, Mansuri S, Ali M, et al. Stress Responses Elicited by Misfolded Proteins Targeted to Mitochondria. J Mol Biol. 2022;434:167618.
[34] Rezazadeh D, Norooznezhad AH, Mansouri K, Jahani M, Mostafaie A, Mohammadi MH, et al. Rapamycin Reduces Cervical Cancer Cells Viability in Hypoxic Condition: Investigation of the Role of Autophagy and Apoptosis. Onco Targets Ther. 2020;13:4239-47.
[35] Lazarou M, Sliter DA, Kane LA, Sarraf SA, Wang C, Burman JL, et al. The ubiquitin kinase PINK1 recruits autophagy receptors to induce mitophagy. Nature. 2015;524:309-14.

[36] Shi J, Fung G, Deng H, Zhang J, Fiesel FC, Springer W, et al. NBR1 is dispensable for PARK2-mediated mitophagy regardless of the presence or absence of SQSTM1. Cell Death Dis. 2015;6:e1943.
[37] Wu Z, Tantray I, Lim J, Chen S, Li Y, Davis Z, et al. MISTERMINATE Mechanistically Links Mitochondrial Dysfunction with Proteostasis Failure. Mol Cell. 2019;75:835-48 e8.
[38] Crowley LC, Christensen ME, Waterhouse NJ. Measuring Mitochondrial Transmembrane Potential by TMRE Staining. Cold Spring Harb Protoc. 2016;2016.
[39] Lee MK, Stirling W, Xu Y, Xu X, Qui D, Mandir AS, et al. Human alpha-synuclein-harboring familial Parkinson's disease-linked Ala-53 --> Thr mutation causes neurodegenerative disease with alpha-synuclein aggregation in transgenic mice. Proc Natl Acad Sci U S A. 2002;99:8968-73.
[40] Stefanis L. alpha-Synuclein in Parkinson's disease. Cold Spring Harb Perspect Med. 2012;2:a009399.
[41] Kimura S, Noda T, Yoshimori T. Dissection of the autophagosome maturation process by a novel reporter protein, tandem fluorescent-tagged LC3. Autophagy. 2007;3:452-60.
[42] Rozenknop A, Rogov VV, Rogova NY, Lohr F, Guntert P, Dikic I, et al. Characterization of the interaction of GABARAPL-1 with the LIR motif of NBR1. J Mol Biol. 2011;410:477-87.
[43] Birgisdottir AB, Lamark T, Johansen T. The LIR motif - crucial for selective autophagy. J Cell Sci. 2013;126:3237-47.
[44] Johansen T, Lamark T. Selective Autophagy: ATG8 Family Proteins, LIR Motifs and Cargo Receptors. J Mol Biol. 2020;432:80-103.
[45] Quinet G, Genin P, Ozturk O, Belgareh-Touze N, Courtot L, Legouis R, et al. Exploring selective autophagy events in multiple biologic models using LC3-interacting regions (LIR)-based molecular traps. Sci Rep. 2022;12:7652.
[46] Wild P, McEwan DG, Dikic I. The LC3 interactome at a glance. J Cell Sci. 2014;127:3-9.
[47] Kim YY, Um JH, Yoon JH, Kim H, Lee DY, Lee YJ, et al. Assessment of mitophagy in mt-Keima Drosophila revealed an essential role of the PINK1-Parkin pathway in mitophagy induction in vivo. FASEB J. 2019;33:9742-51.
[48] Liu YT, Sliter DA, Shammas MK, Huang X, Wang C, Calvelli H, et al. Mt-Keima detects PINK1-PRKN mitophagy in vivo with greater sensitivity than mito-QC. Autophagy. 2021;17:3753-62.
[49] Sun N, Malide D, Liu J, Rovira, II, Combs CA, Finkel T. A fluorescence-based imaging method to measure in vitro and in vivo mitophagy using mt-Keima. Nat Protoc. 2017;12:1576-87.

Figure Legends

Figure 1. E3 ubiquitin ligase Parkin facilitates the mitochondrial recruitment of ANKZF1 on chemical stress-induced damaged mitochondria. A. Schematic representation of ANKZF1 domain map. From N-terminal of the protein, there is a Leucine Rich Sequence (LRS) followed by a Zinc-finger domain (ZnF). After ZnF, there is a putative Mitochondrial Targeting Domain (MTD) the exact boundary of MTD remains elusive yet. MTD is followed by two Ankyrin repeats (Ank), followed by a coiled-coil domain, a yet

uncharacterized domain (shown as an orange box), and a VCP-interacting motif (VIM). The numbers mentioned indicate the number of amino acids in the primary sequence of the protein. **B.** Cellular distribution of ANKZF1-GFP is shown by imaging of transfected HeLa cells by confocal microscopy. MitoTracker-Red was used to stain the mitochondrial network. Right most panel is the merged panel of both red and green panels. **C.** ANKZF1 localization is shown during mitochondrial stress by various small molecule stressors (CCCP, H_2O_2, rotenone, Na-Azide, rapamycin and paraquat). In all stresses, ANKZF1 exhibits a diffused cytosolic localization except few punctate structures in rapamycin stress. **D.** ANKZF1 is recruited as punctate forms on mitochondria during CCCP, and rapamycin-induced stress in the presence of Parkin overexpression in HeLa cells, Line-scan profile of fluorescence intensity of Mito-BFP, ANKZF1-GFP, and mCherry-Parkin are shown as blue, green, and red lines respectively, at the bottom of Rapamycin and CCCP treated condition. **E**. Pearson's correlation coefficient of co-localization of mCherry-Parkin and ANKZF1-GFP was calculated in the non-stress control (Mito-BFP) conditions, and during rapamycin and CCCP-treated conditions. Values represent means ± SEM, N = 3. Images of at least 50 cells were considered for quantification. One-way ANOVA with Dunnett multiple comparison test was performed to determine the mean differences, **** indicates $P < 0.0001$.

Figure 2. Generation of model of mitochondria-specific single misfolded/aggregated protein-induced proteotoxic stress, in human cells. A. Schematic representation of model stressor proteins, A53T α-synuclein, and PMD (Protein with Misfolded Domain)-fused to GFP, targeted to mitochondria. MTS denotes Mitochondrial Targeting Sequence. **B.** Expression and localization of mitochondria-targeted A53T α-synuclein and PMD proteins in HeLa cells were checked by imaging using confocal microscopy. Mitochondria-targeted mCherry (Mito-mCherry) was used as a mitochondrial marker Line-scan profile of fluorescence intensity of mitochondria-targeted GFP-tagged proteins (Mito-GFP, Mito-A53T Syn-GFP, and Mito-PMD-GFP) and Mito-mCherry are shown in green and red lines, respectively. **C**. Co-localization analysis of GFP-tagged control/stressor protein with Mito-

mCherry by Mander's overlap shows more than 90% co-localization score of these stressor proteins to mitochondrial marker, exhibiting correct mitochondrial targeting. Values represent means ± SEM (N = 3). **D and E.** Expression of both of these stressor proteins in mitochondria leads to increased mitochondrial fragmentation. However, PMD expression leads to significantly enhanced mitochondrial fragmentation, where the size of mitochondria is reduced to less than one-third of the length of healthy mitochondria. Values in panel E represent mitochondria mean branch lengths in µm ± SEM (N=3). One-way ANOVA with Dunnett multiple comparison test was performed to determine the mean differences in both plot B and F, ****P < 0.0001.

Figure 3. Parkin also assists in recruitment of ANKZF1 on severely fragmented mitochondria during mitochondrial proteotoxic stress. A-B. Any changes in autophagic flux due to proteotoxic stress in mitochondria by expressing the stressor proteins, A53T α-synuclein or PMD, was further confirmed by expressing the fluorescent reporter protein mRFP-GFP tandem fluorescently-tagged LC3 (tfLC3). GFP and RFP fluorescence intensity of LC3 puncta were measured and GFP/RFP of each puncta were calculated and plotted as bar plots (B), as explained in the main text, mitochondrial proteotoxic stress leads to reduced GFP/RFP ratio of tfLC3 suggesting significantly increased overall autophagic flux during mitochondrial targeted proteotoxic stress in comparison to the control condition. Values represent means ± SEM (N= 3). One-way ANOVA with Dunnett multiple comparison test was performed to determine the mean differences, ***P < 0.001, ****P < 0.0001**. C and D.** ANKZF1-GFP was co-expressed with A53T α-synuclein-BFP or PMD-BFP in the absence (panel C) or in the presence of mCherry-Parkin (panel D) in HeLa cells. Without any stress (control protein BFP is expressed in mitochondria), ANKZF1 shows diffused cytosolic localization (Upper row panel C). ANKZF1 forms some punctate foci during A53T-α-synuclein (middle row panel C) or PMD-induced stress (lower row panel C) in mitochondria. Line-scan profile of fluorescence intensity of BFP-tagged stressor proteins (Mito-A53T Syn BFP and Mito-PMD BFP) and ANKZF1-GFP are shown in blue and green colors,

respectively (panel C). Similarly, in the presence of Parkin, along with blue and green lines, mCherry-Parkin fluorescence is represented as a red line (panel D) showing merged peaks suggesting co-localization. ANKZF1 puncta are recruited over mitochondria during mitochondrial proteotoxic stress even in the absence of Parkin (panel C). However, the recruitment of ANKZF1 is significantly increased when Parkin is overexpressed in HeLa cells (Panel D), suggesting ANKZF1 recruitment on stressed mitochondria is facilitated by Parkin. **E.** Pearson's correlation coefficient of co-localization was calculated and plotted for Parkin and ANKZF1 puncta during unstressed control (Mito-BFP) condition, Mito-A53T Syn-BFP and Mito-PMD-BFP induced stress conditions, Values represent means ± SEM, (N= 3), one-way ANOVA with Dunnett multiple comparison test was performed to determine the mean differences, ****P < 0.0001. **F.** ANKZF1 puncta count per cell in the absence and presence of Parkin during control conditions (mitochondria expressing Mito-BFP) and proteotoxic stress conditions (mitochondria expressing Mito-A53T Syn-BFP and Mito-PMD-BFP), shows a significant increase in ANKZF1 puncta formation in presence of Parkin during proteotoxic stress condition. Values represent means ± SEM, (N= 3), paired t-test was performed to determine pairwise mean differences, ns is non-significant, **P < 0.01, ***P < 0.001.

Figure 4. ANKZF1 shows interaction with Parkin and LC3 during mitochondrial proteotoxic stress and CCCP-induced stress. A. ANKZF1-GFP and RFP-LC3 were co-expressed in HeLa cells along with Mito-BFP, A53T-α-synuclein-BFP, and PMD-BFP. In the control panel (Mito-BFP), ANKZF1 shows diffused cytosolic expression, and low LC3 puncta formation was observed, but in stressed conditions, lower two panels (A53T α-synuclein BFP and PMD BFP) a high number of RFP-LC3 puncta formation and ANKZF1 puncta formation was observed. Line-scan profile of fluorescence intensity of BFP-tagged protein constructs (Mito-A53T Syn BFP, and Mito-PMD BFP) targeted to mitochondria shown in blue and ANKZF1 GFP shown in green and RFP-LC3 was indicated in the red color profile. **B.** Pearson's correlation coefficient of co-localization was calculated for RFP-tagged LC3 puncta and GFP-tagged ANKZF1 during unstressed control (Mito-BFP), Mito-A53T-Syn-

BFP, and Mito-PMD-BFP conditions. Values represent means ± SEM, N=3, and one-way ANOVA with Dunnett multiple comparison test was performed to determine the mean differences, ****P < 0.0001. **C.** ANKZF1-BFP, GFP-Parkin, and RFP-LC3 were co-expressed along with Mito-PMD, showing puncta of ANKZF1, Parkin, and LC3 are getting co-localized. The zoomed panel shows the highly co-localized phagophore like structures of ANKZF1, Parkin, and LC3. **D.** Co-immunoprecipitation of mCherry-Parkin and LC3 with ANKZF1-GFP was performed during CCCP-treated depolarization and PMD-induced proteotoxic stress conditions. Left panel shows the 5% load of whole cell lysate before binding to Protein A/G Sepharose beads, while right panel shows immunoprecipitated proteins (IP) with pre-immune antisera and anti-GFP antibody. Blots were probed with anti-GFP (top), anti-Parkin (middle) and anti-LC3 (bottom) antibodies (Supplementary Table 2).

Figure 5. ANKZF1 sequence contains six putative LC3-Interacting Regions (LIRs), and LIR-4 (333-336 residues) is indispensable for LC3-interaction. **A.** Multiple sequence analysis (MSA) of some of the known mitophagy/autophagy adaptor/receptor proteins shows the presence of a conserved LIR (LC3 interacting region) motifs. B. ANKZF1 sequence analysis shows the presence of six different probable LIR motifs consisting of similar sequence like known adaptors/receptors, named as LIR1 to LIR6. **C.** MSA of ANKZF1 sequence from different mammals shows the presence of conservation of LIR2, LIR3, LIR4 and LIR6. **D.** Schematic overview to depict the distribution of 6 LIR-like motifs in ANKZF1 full-length protein sequence, three truncation mutants of ANKZF1 (Δ210, Δ330, Δ370) were designed to screen the probable functional LIR motifs crucial for interaction with LC3. Schematic representation of truncation mutants show the presence and absence of LIRs in these three mutants compared to the full-length wild type ANKZF1 protein (ANKZF1 FL). **E.** ANKZF1 recruitment and interaction with LC3 during PMD-induced mitochondrial proteotoxic stress were checked after expressing the truncation mutants of ANKZF1. ANKZF1-FL shows punctate foci that co-localize with RFP-LC3 puncta during proteotoxic stress (panel E, upper row). Δ210-ANKZF1, Δ330-ANKZF1 truncation mutants also show similar behavior and

significantly co-localize with LC3 puncta (panel E, second and third rows from the top) like the full-length protein. Δ370-ANKZF1 shows a diffused cytosolic pattern indicating no interaction with LC3. Line-scan profile of fluorescence intensity of RFP-LC3 puncta and WT-ANKZF1/ Δ210-ANKZF1/Δ330-ANKZF1 puncta shows merged intensity peak suggesting co-localization. In contrast, Δ370-ANKZF1-GFP puncta and RFP-LC3 puncta peaks do not merge, suggesting the absence of interaction. ANKZF1 peaks are shown in green and LC3 peaks are shown in red. **F.** Pearson's correlation coefficient of co-localization was calculated and plotted for LC3 puncta and ANKZF1 (WT-ANKZF1, Δ210-ANKZF1, Δ330-ANKZF1, and Δ370-ANKZF1) puncta during Mito-PMD BFP induced stress conditions, Values represent means ± SEM, N=3, one-way ANOVA with Dunnett multiple comparison test was performed to determine the mean differences, ****$P < 0.0001$. **G**. ANKZF1 LIR mutants, F333A-L336A, W366A-V369A, and W495A-L498A fused with GFP were co-transfected with RFP-LC3 in HeLa cells along with PMD-BFP. W366A-V369A and W495A-L498A mutants of ANKZF1 show interaction and co-localization with RFP-LC3 like the wild type ANKZF1 (middle and lower panel), F333A-L336A mutant of ANKZF1 during PMD induced stress is not showing any co-localization with RFP-LC3 (top panel). Line-scan profile of fluorescence intensity of mutant ANKZF1-GFP and RFP LC3 puncta shows merged intensity peak suggesting co-localization.

Figure 6. Cells deleted of ANKZF1 show compromised mitophagy during mitochondrial proteotoxic stress. A. Schematic representation of CRISPR-Cas9 mediated *ANKZF1* knockout (KO) generation. Sequence of two single guide RNAs (sgRNAs) that were used in combination are shown in the schematic. **B.** Confirmation of *ANKZF1* knockout cells by western blot with ANKZF1-specific antibody. Actin was used as a loading control. **C.** The mitophagy efficiency of WT HeLa cells and *ANKZF1* KO cells were compared by using pH dependent Mt-Keima protein as explained in the results. KO cells showed functional mitophagy events but significantly decreased mitophagy events in

comparison to WT HeLa cells during PMD-induced mitochondrial proteotoxic stress. **D.** Ratiometric analysis of Keima560 vs Keima488 fluorescence intensity, PMD expressed WT-Hela cells showing high 560/488 ratio in comparison to the KO cells corresponding high mitophagy rate. **E.** Average mitophagy events per cell during control and stressed conditions in WT-HeLa cells and *ANKZF1* knockout cells were assessed by counting the red signals (autophago-lysosome) from the merged panel of Mt-Keima (panel C). Red-only vesicles are shown with white arrowheads in the inset of the merged panel (right most column of panel C). Values represent means ± SEM, (N =3). Unpaired t-test was performed to determine the mean difference, ***P < 0.001.

Figure 7: An illustrated summary of ANKZF'1 role as a mitophagy adaptor protein.

Figure 7 shows a summary of ANKZF1's role as mitophagy adaptor protein. The box shows the interaction of LC3-Interacting Regions (LIR) of ANKZF1 with LC3 on the growing phagophore membrane. The flow diagram on the left shows the stepwise process of mitophagy induction and clearance of damaged mitochondria during proteotoxic stress in the organelle. Here, ANKZF1 has been shown to act as a mitophagy adaptor, which helps in autophagosome formation surrounding the damaged mitochondria by interacting with ubiquitinated mitochondrial outer membrane proteins and LC3 on the growing phagophore membrane.

Figure 1

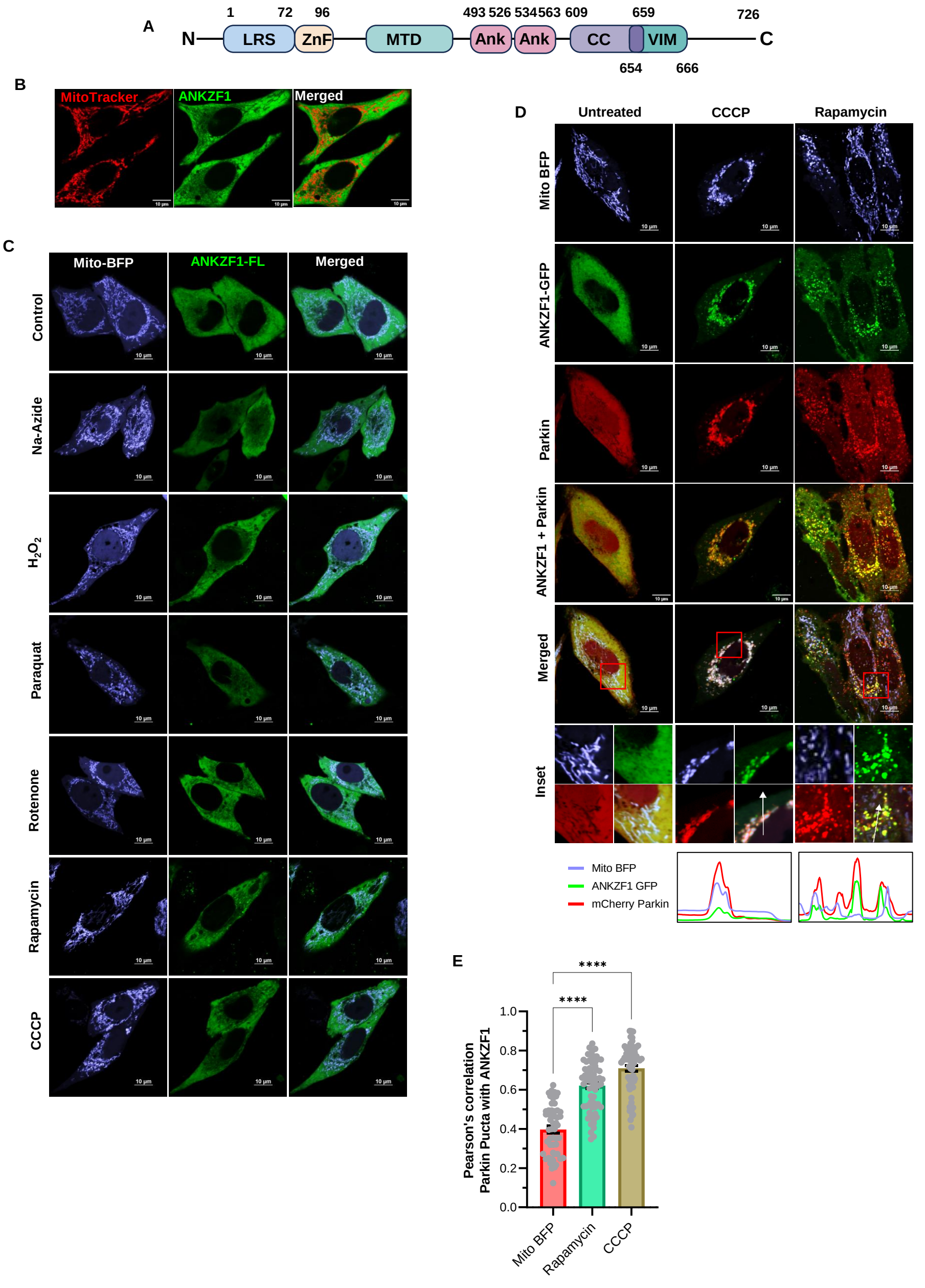
A
N
1
72
96
493 526 534563 609
659
726
LRS
ZnF
MTD
Ank
Ank
CC
VIM
C
654
666
B
MitoTracker
ANKZF1
Merged
C
Mito-BFP
ANKZF1-FL
Merged
Control
Na-Azide
H2O2
Paraquat
Rotenone
Rapamycin
CCCP
10 µm
D
Untreated
CCCP
Rapamycin
Mito BFP
ANKZF1-GFP
Parkin
ANKZF1 + Parkin
Merged
Inset
Mito BFP
ANKZF1 GFP
mCherry Parkin
E
Pearson's correlation
Parkin Pucta with ANKZF1
1.0
0.8
0.6
0.4
0.2
0.0
****
****
Mito BFP
Rapamycin
CCCP

Figure 2

A

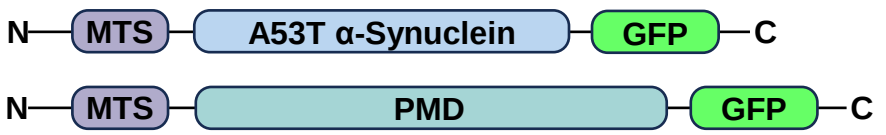

B

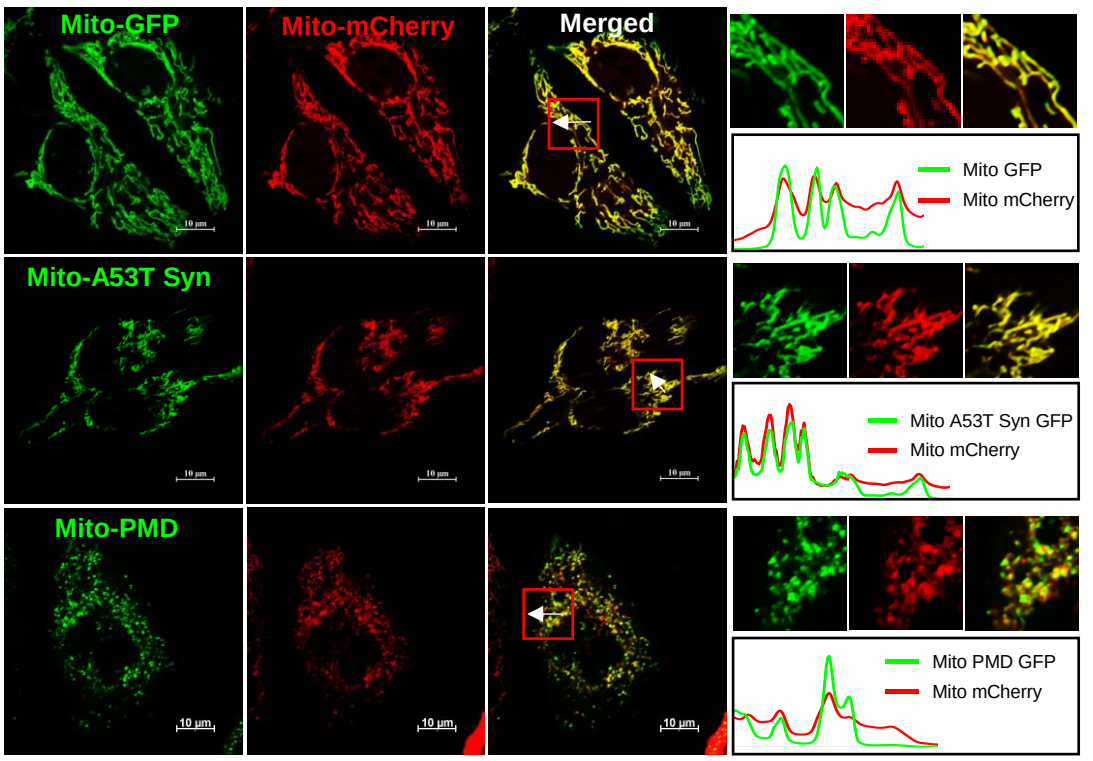

C

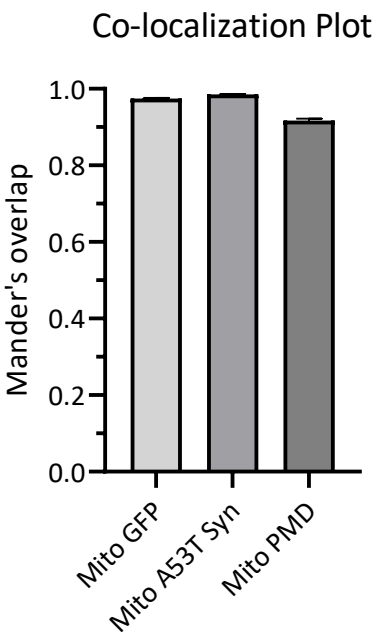

D

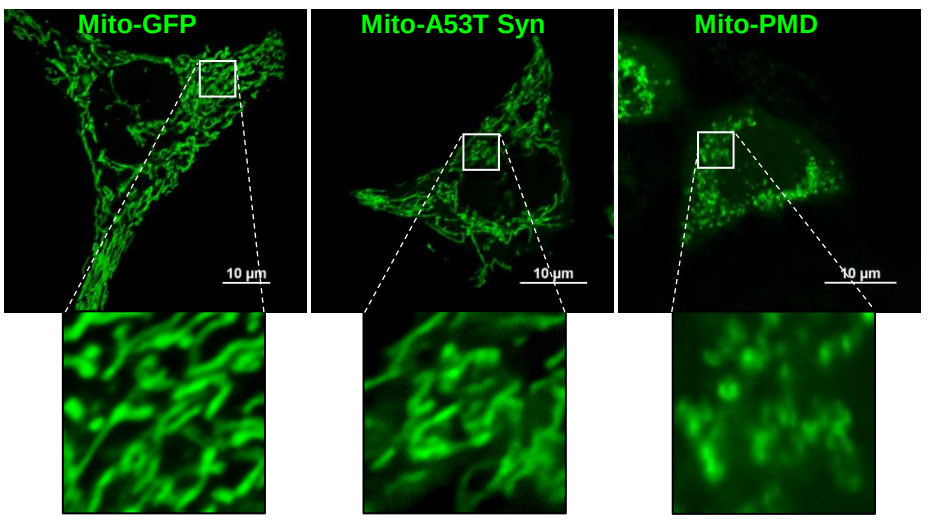

E

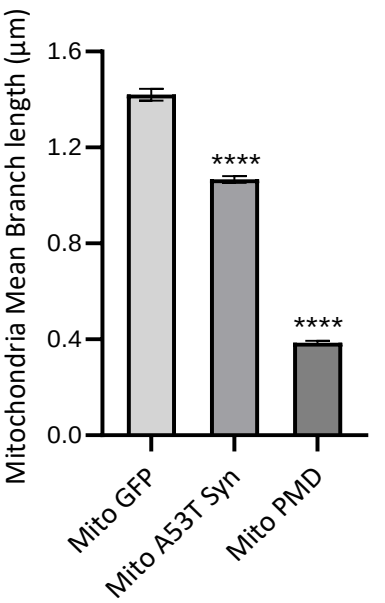

Figure 3

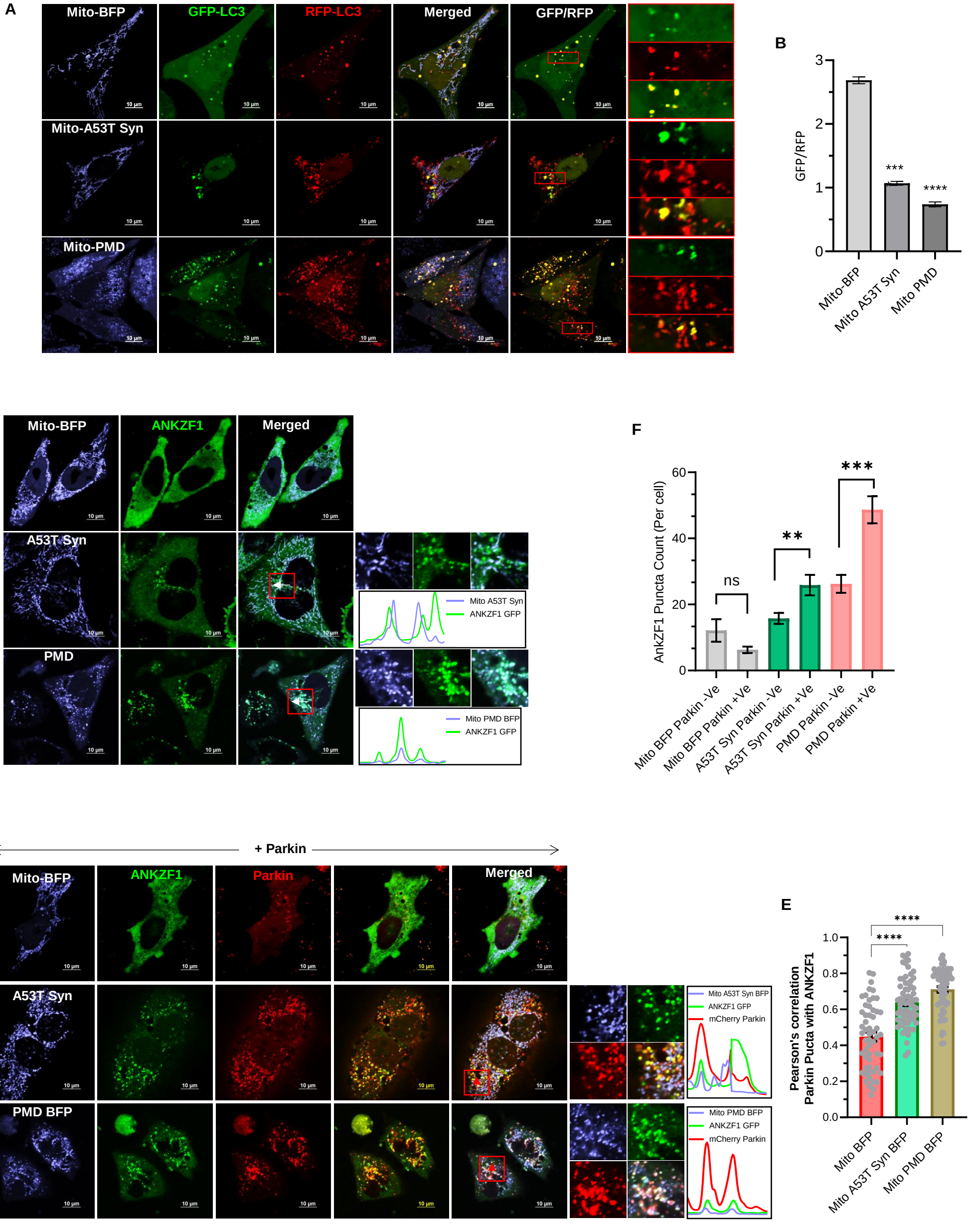
A
Mito-BFP
GFP-LC3
RFP-LC3
Merged
GFP/RFP
Mito-A53T Syn
Mito-PMD
10 µm
B
GFP/RFP
***
****
Mito-BFP
Mito A53T Syn
Mito PMD
C
Mito-BFP
ANKZF1
Merged
A53T Syn
PMD
Mito A53T Syn
ANKZF1 GFP
Mito PMD BFP
F
AnkZF1 Puncta Count (Per cell)
ns
**
***
Mito BFP Parkin -Ve
Mito BFP Parkin +Ve
A53T Syn Parkin -Ve
A53T Syn Parkin +Ve
PMD Parkin -Ve
PMD Parkin +Ve
D
+ Parkin
Mito-BFP
ANKZF1
Parkin
Merged
A53T Syn
PMD BFP
Mito A53T Syn BFP
ANKZF1 GFP
mCherry Parkin
Mito PMD BFP
E
Pearson's correlation
Parkin Pucta with ANKZF1
****
Mito BFP
Mito A53T Syn BFP
Mito PMD BFP

Figure 4

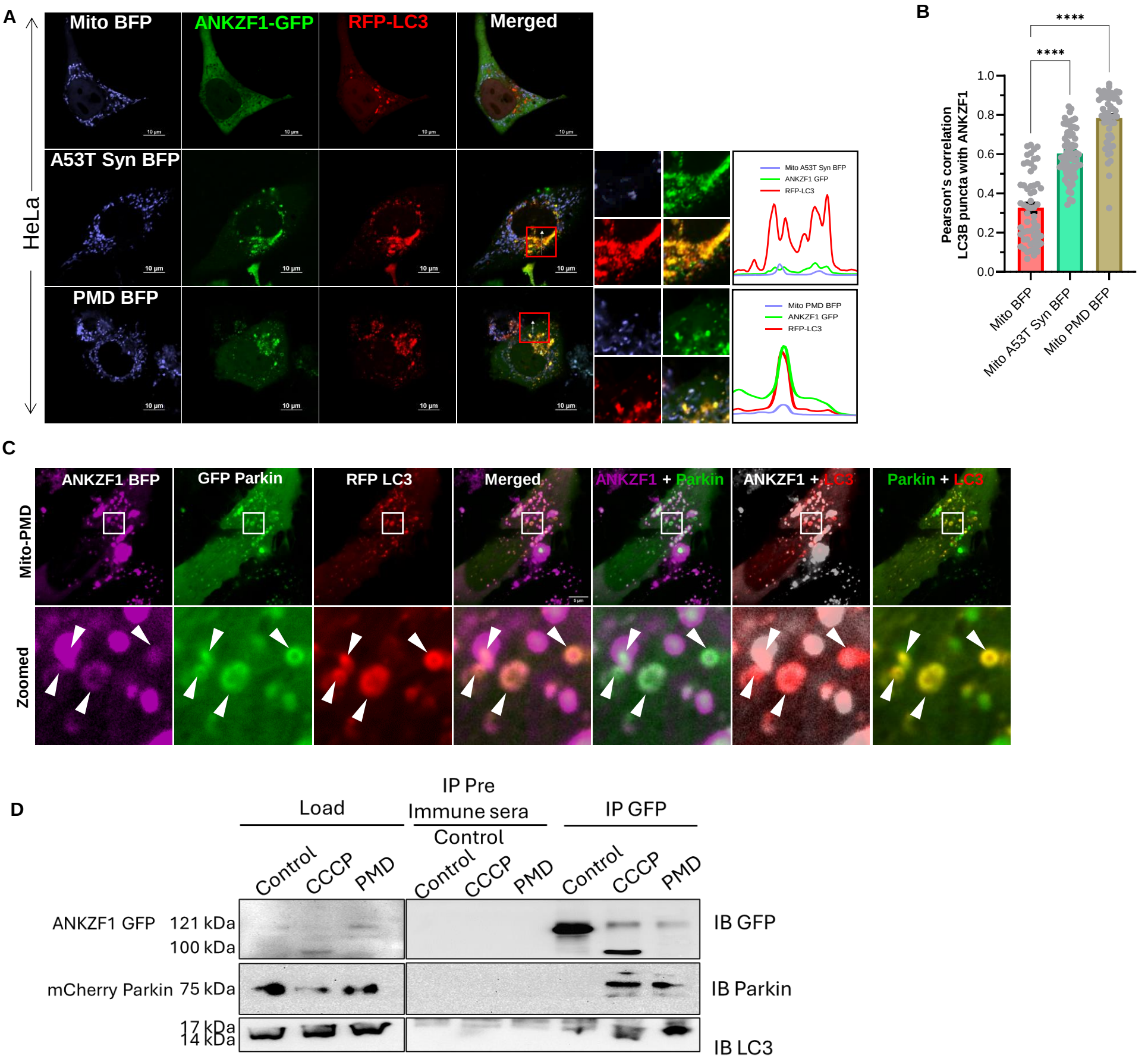
A
Mito BFP
ANKZF1-GFP
RFP-LC3
Merged
A53T Syn BFP
PMD BFP
HeLa
10 µm
Mito A53T Syn BFP
ANKZF1 GFP
RFP-LC3
Mito PMD BFP
B
Pearson's correlation LC3B puncta with ANKZF1
****
****
1.0
0.8
0.6
0.4
0.2
0.0
Mito BFP
Mito A53T Syn BFP
Mito PMD BFP
C
Mito-PMD
Zoomed
ANKZF1 BFP
GFP Parkin
RFP LC3
Merged
ANKZF1 + Parkin
ANKZF1 + LC3
Parkin + LC3
D
Load
IP Pre Immune sera
Control
IP GFP
Control
CCCP
PMD
ANKZF1 GFP
121 kDa
100 kDa
mCherry Parkin
75 kDa
17 kDa
14 kDa
IB GFP
IB Parkin
IB LC3

Figure 5

A

```
NIX/BNIP3 AGLNSSWVELPMNSSN   45
    BNIP3 ESLQGSWVELHFSNNG   29
      p62 SGGDDDWTHLSSKEVD   347
Optineurin GSSEDSFVEIRMAEGE  187
     NBR1 SASSEDYIIILPECFD   741
   Ambra1 SGVEYYWDQLNETVFT   1058
   FUNDC1 ESDDDSYEVLDLTEYA   27
     ULK1 SCDTDDFVMVPAQFPG   376
```

LC3 interacting region (LIR) W/F/Y XX L/I/V

B

		W/Y/F	X	X	L/I/V	
LIR #1	151	F	E	K	L	154
LIR #2	178	Y	R	C	V	181
LIR #3	272	Y	K	D	V	275
LIR #4	333	F	Q	E	L	336
LIR #5	366	W	K	T	V	369
LIR #6	495	W	N	A	L	498

C

	LIR 1	LIR 2	LIR 3	LIR 4	LIR 5	LIR 6
Guinea_Pig	....CERP....	YRCV....	YKDV....	FREL....	WKTM....	WDIL....
Golden_Hamster	....FEKP....	YRCV....	YKDV....	FGEL....	WKPV....	WDML....
Mouse	....SEKP....	YRCV....	YKDV....	FGEL....	WKPV....	WDTL....
Rat	....SEKP....	YRCV....	YKDV....	FGEL....	CKPV....	WDML....
Bovine	....LEKP....	YRCV....	YKEV....	FQEL....	RKRV....	WDVL....
Rabbit	....SETP....	YRCV....	CKDV....	FREL....	WKTA....	WAGL....
Human	....FEKL....	YRCV....	YKDV....	FQEL....	WKTV....	WNAL....
	*	****	*:*	* **	*	* *

D

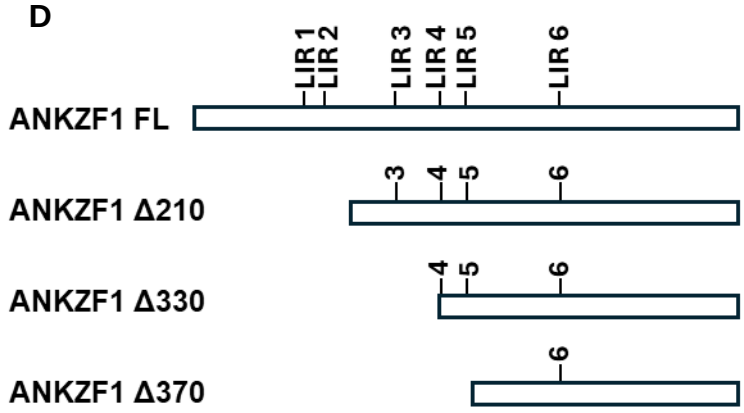

E

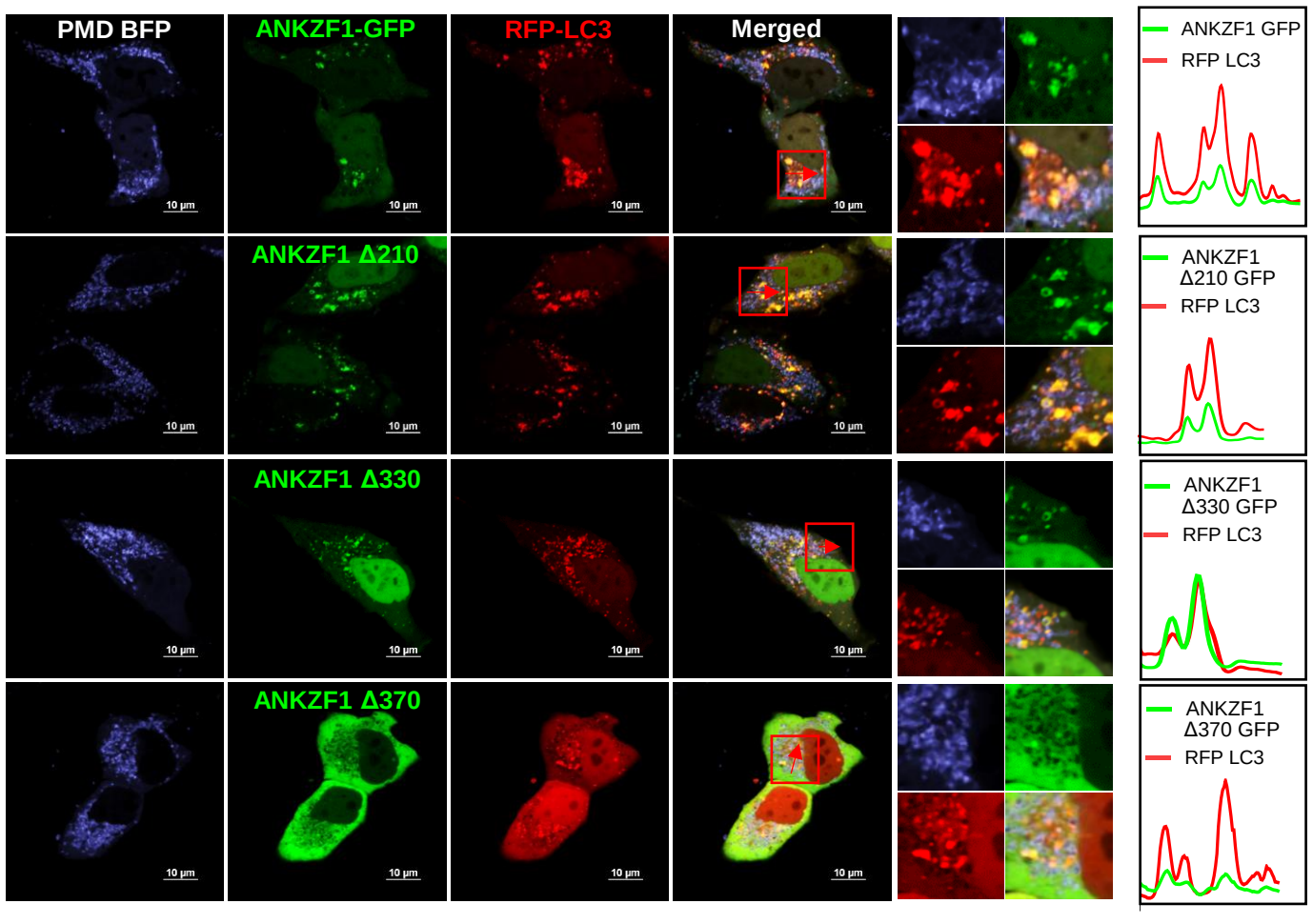

F

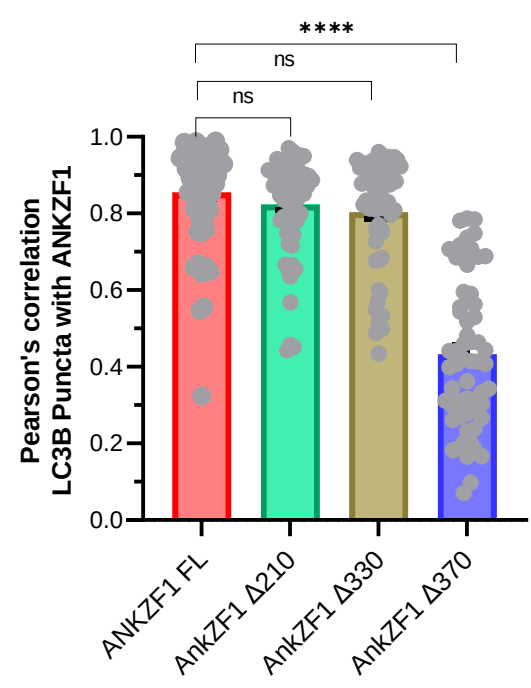

G

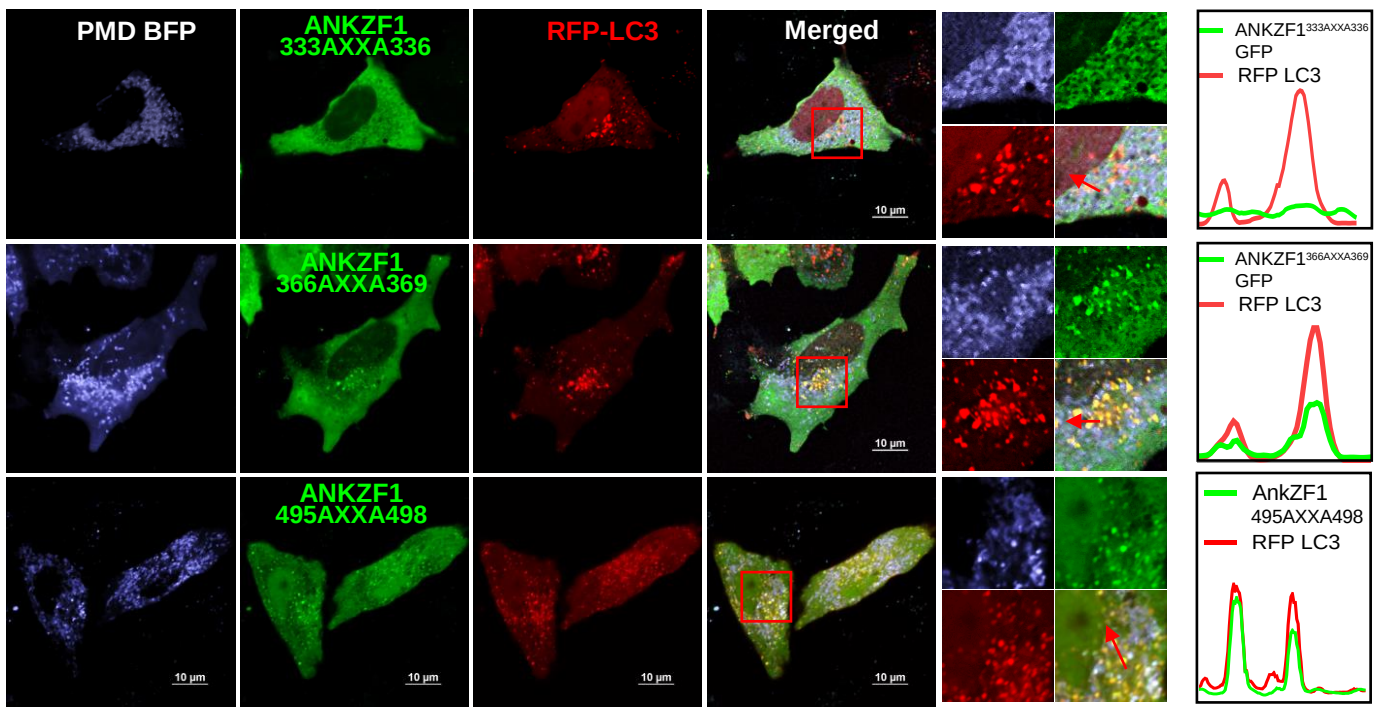

Figure 6

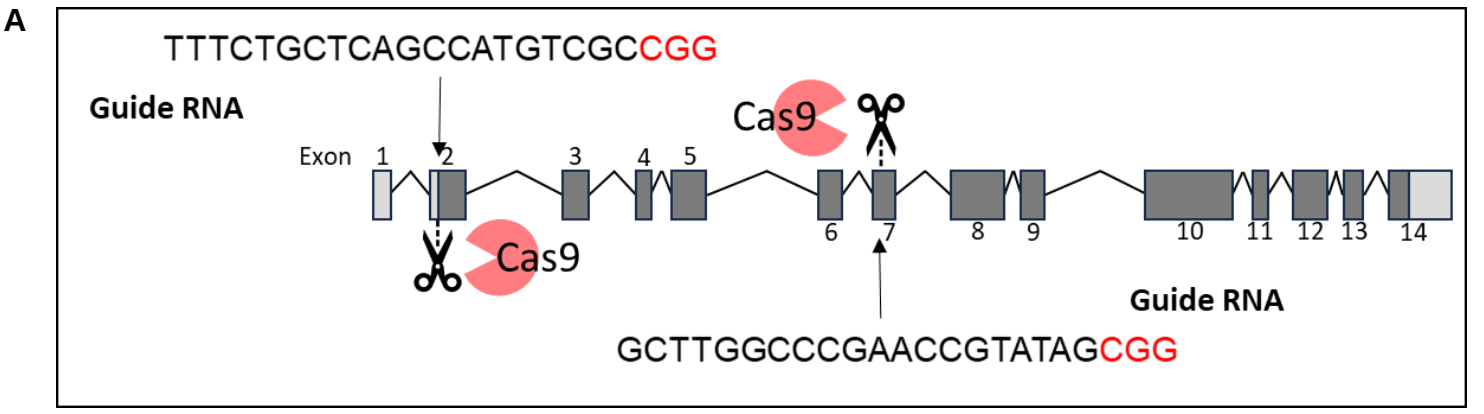
A
TTTCTGCTCAGCCATGTCGCCGG
Guide RNA
Exon
1
2
3
4
5
6
7
8
9
10
11
12
13
14
Cas9
Cas9
Guide RNA
GCTTGGCCCGAACCGTATAGCGG

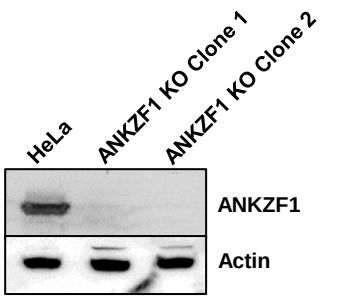
B
HeLa
ANKZF1 KO Clone 1
ANKZF1 KO Clone 2
ANKZF1
Actin

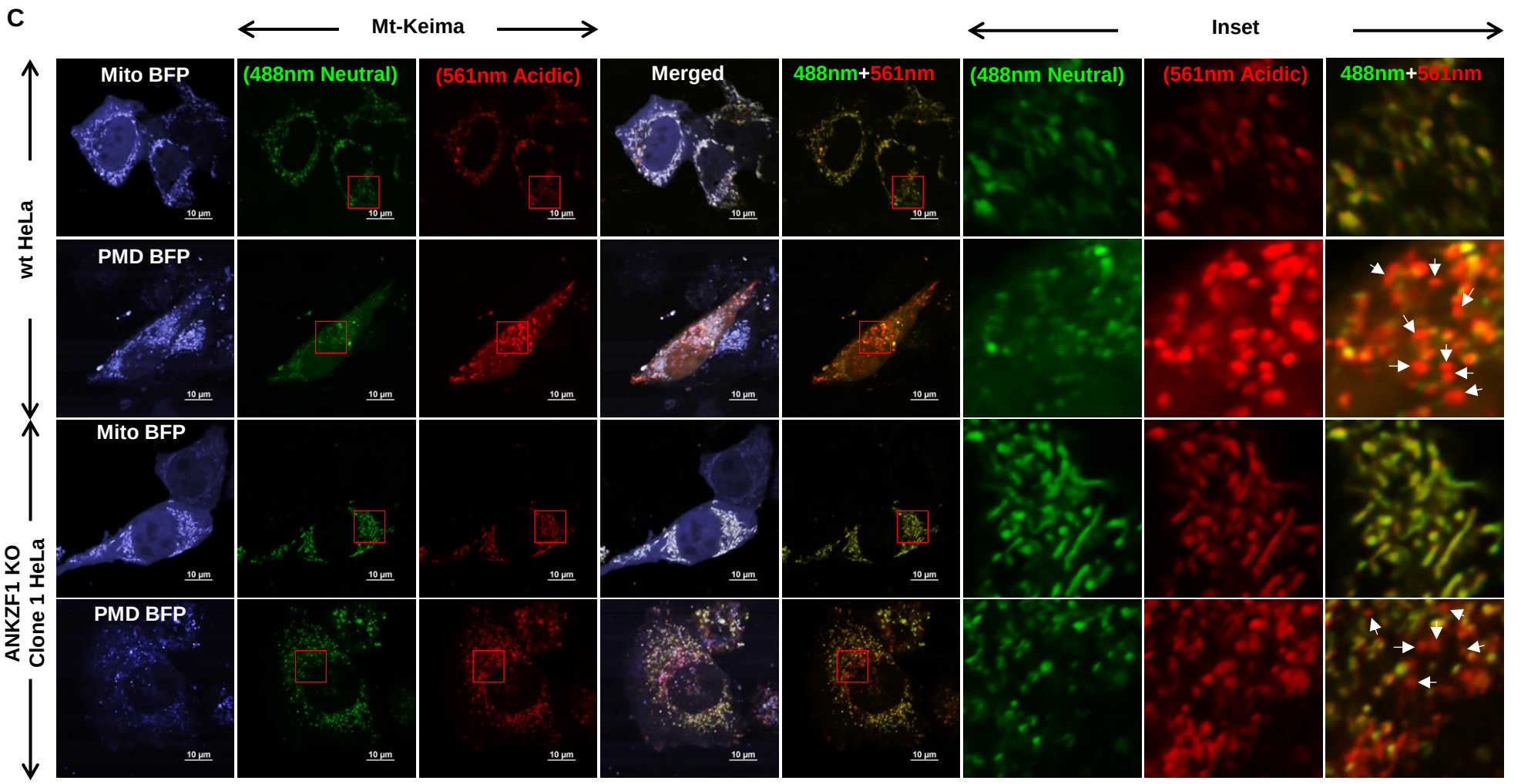
C
Mt-Keima
Inset
Mito BFP
(488nm Neutral)
(561nm Acidic)
Merged
488nm+561nm
(488nm Neutral)
(561nm Acidic)
488nm+561nm
wt HeLa
PMD BFP
Mito BFP
PMD BFP
ANKZF1 KO Clone 1 HeLa
10 µm

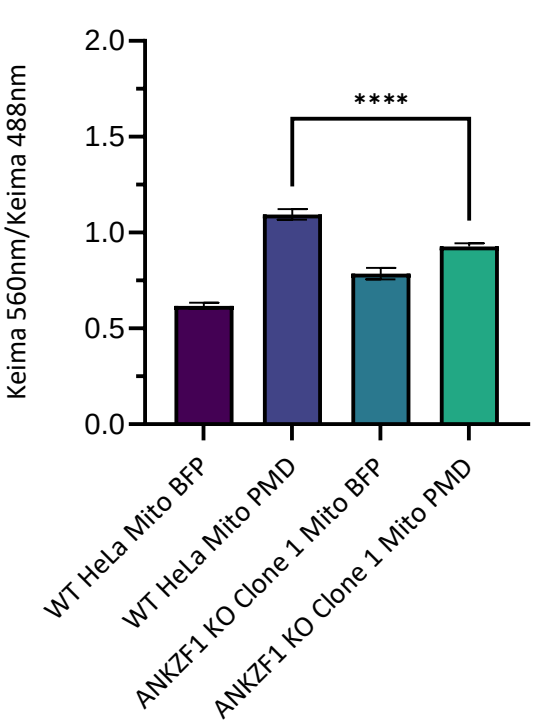
D
Keima 560nm/Keima 488nm
2.0
1.5
1.0
0.5
0.0
****
WT HeLa Mito BFP
WT HeLa Mito PMD
ANKZF1 KO Clone 1 Mito BFP
ANKZF1 KO Clone 1 Mito PMD

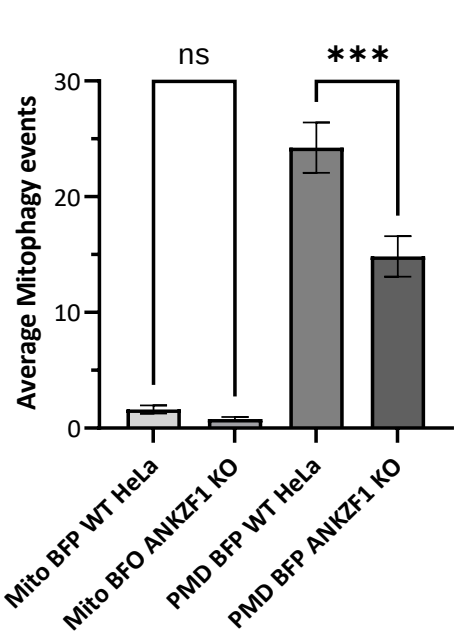
E
Average Mitophagy events
30
20
10
0
ns
***
Mito BFP WT HeLa
Mito BFO ANKZF1 KO
PMD BFP WT HeLa
PMD BFP ANKZF1 KO
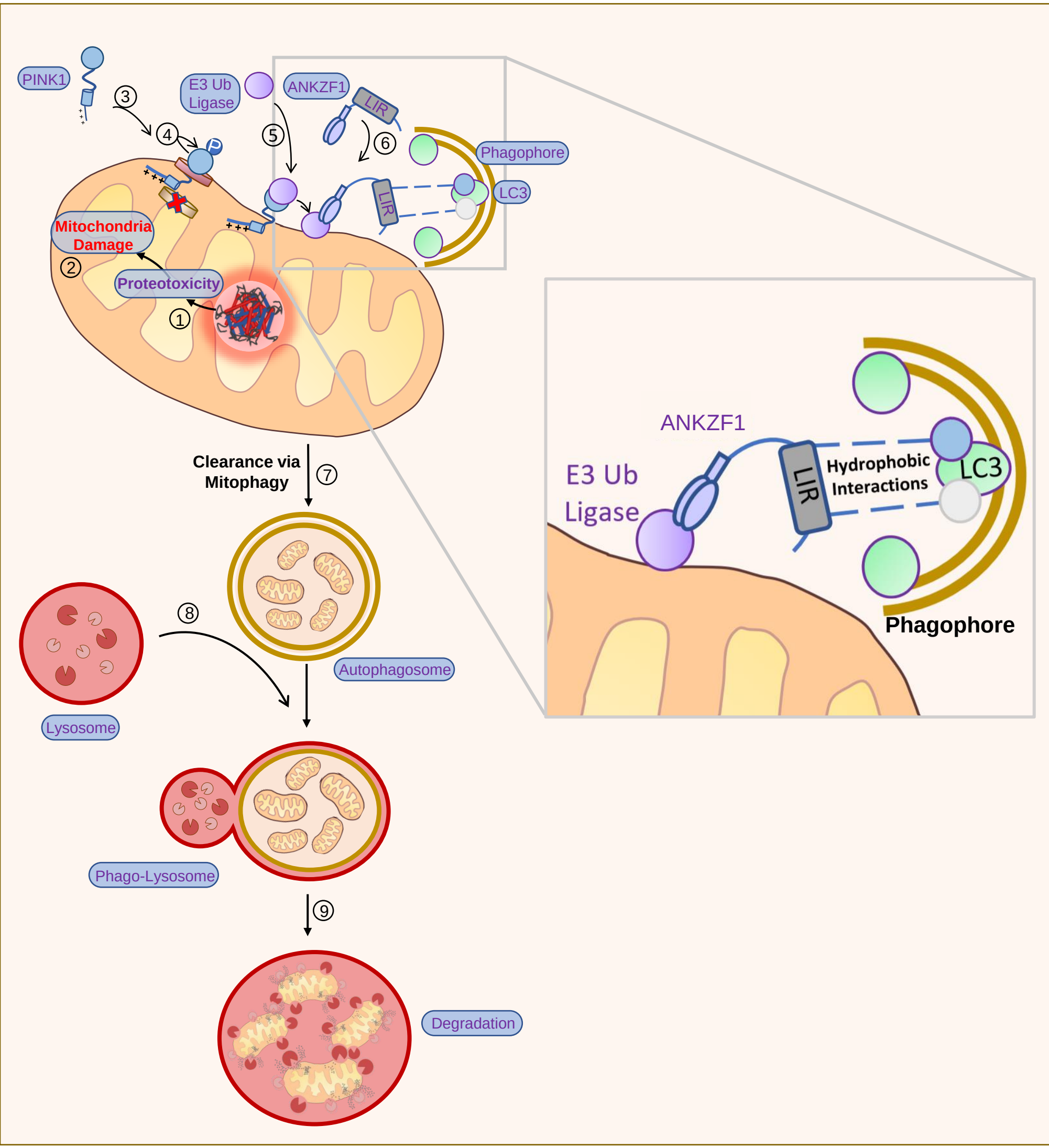
Figure 7. Summary: ANKZF1 helps in the clearance of damaged mitochondria via PINK1/Parkin and LC3-mediated mitophagy